Spectrochimica Acta Part A: Molecular and Biomolecular Spectroscopy 265 (2022) 120260

Contents lists available at ScienceDirect

Spectrochimica Acta Part A: Molecular and Biomolecular Spectroscopy

journal homepage: www.elsevier.com/locate/saa

# Enriching the knowledge of Ostia Antica painted fragments: a multi-methodological approach

Bracci Susanna [a,*,1], Cantisani Emma [a], Conti Claudia [b], Magrini Donata [a], Vettori Silvia [a], Tomassini Paolo [c], Marano Martina [d]

[a] Institute of Heritage Science – National Council of Research, Via Madonna del Piano, 10, 50019 Florence, Italy
[b] Institute of Heritage Science – National Council of Research, Via Cozzi, 53, 20125 Milan, Italy
[c] École française de Rome, Centro Studi Pittura Romana Ostiense, Italy
[d] Fonds de la Recherche Scientifique (FNRS), Université catholique de Louvain, Centro Studi Pittura Romana Ostiense, Italy

## HIGHLIGHTS

- Scientific knowledge of the palette and technique of Roman wall paintings of Ostia Antica.
- Use of optimized protocol integrating both non-invasive and microinvasive techniques.
- Analogies and differences in the materials employed correlated to the different styles.
- An important source of information for future research especially for the wall paintings still in place.

## GRAPHICAL ABSTRACT

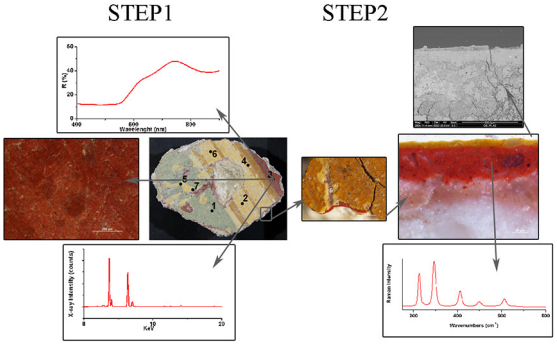


## ARTICLE INFO

*Article history:*
Received 20 February 2021
Received in revised form 16 July 2021
Accepted 3 August 2021
Available online 13 August 2021

*Keywords:*
Roman wall paintings
Pigments
Multi-analytical approach
Non-invasive analytical techniques
Optimized analytical approach

## ABSTRACT

This paper presents the study of selected painted fragments from different contexts of Ostia Antica city, dating between 2nd century BCE and the end of the 1st century CE. The aim is to identify the raw materials used and to understand the execution techniques through a non-invasive protocol including techniques based either on multiband imaging (Visible-VIS, Ultraviolet induced Luminescence - UVL and Visible Induced Luminescence - VIL) and single spot analyses (Fiber Optic Reflectance Spectroscopy-FORS and portable X-Ray Fluorescence spectrometry - XRF). The most representative and interesting fragments were sampled for further studies with laboratory techniques such as optical microscopy (OM) and electron microscopy (SEM), Fourier Transform Infrared and micro-Raman Spectroscopies (FT-IR and μRaman).

The extensive use of non-invasive techniques, even working on fragments, is proved to be the most robust and effective approach enabling the analysis of a high number of areas, dramatically increasing the statistical meaning of the collected data. The elaboration of such a huge number of data allows highlighting differences and similarities, thus achieving a more realistic overview of the materials composition and addressing the sampling to the more significant and complex areas.



* Corresponding author.
*E-mail address:* susanna.bracci@cnr.it (B. Susanna).

[1] This paper is dedicated to the memory of our beloved friend and colleague who suddenly passed away during this research.

https://doi.org/10.1016/j.saa.2021.120260
1386-1425/

## 1. Introduction

The ancient city of Ostia is one of the most significant archaeological sites in Italy and in the world, by virtue of its exceptional state of conservation and its considerable extension. It is in fact one of the few Roman cities of which the plan is almost entirely known, with its extended road network, its public, religious, commercial and residential buildings and the two harbour basins, considered as the largest port structure in Antiquity.

The peculiarity of Ostia is also the possibility to study the evolution of the city through a very long period of time, as the site was occupied and transformed for a thousand years (4th century BCE – 6th century CE) [1,2]. The many buildings, found during excavations started in the 19th century and continued mostly in the 1930s, have returned a huge quantity of painted wall decorations, found both *in situ* and in a fragmentary state. This makes Ostia a crucial testimony for the study of Roman Wall Painting, as it is one of the only archaeological sites where it is possible to follow the evolution of wall painting during more than seven centuries, from the 2nd century BCE to the 5th century CE [3].

Studying the wall decorations, through a collaborative archaeological and scientific approach, it is therefore possible to reconstruct the historical development of the Ostian wall paintings during time, to trace the evolution of techniques and the workshop practices in the city. This approach throws a new light on several questions: who were the painters operating in the city? Were there any local workshops? Which techniques did they use? How did the technique and practice of Roman painting change during the centuries?

In this paper the focus is on a specific period for the history of Ostia and its paintings from the 2nd century BCE to the 1st century CE (time during which the so-called "Pompeian" Styles develop). For many years, very few testimonies of this period were known in Ostia, due to the fact that most of the city's buildings are dated to the beginning of the 2nd century CE, after a urban, economic and demographic boom that transformed completely the facies of the city, destroying older structures in order to build new, multistoreyed *insulae* [4]. It was only in the 1970s that these older structures were partially investigated by the *Soprintendenza di Ostia*, that carried out stratigraphic excavations deep under the level of the 2nd century buildings, bringing to light a very large quantity of wall paintings in fragments, destroyed and re-used as a filling in the construction layers of the *insulae*. The fragments, long forgotten in the Deposits of Ostia, were recently studied, assembled and recomposed by members of the *Centro studi pittura romana ostiense* (CeSPRO), allowing to reconstruct a large number of painted wall and ceiling decorations of First, Second, Third and Fourth Style [5–13,6–13].

These fragments, although detached from the walls and whose original location is often lost, are extremely important for the knowledge of Ostian wall paintings, as they are the only surviving evidence of the city's pictorial production of the period preceding the large renovation works of the 2nd century CE. They offer a glance of the skills of the painters but also the taste of the population and their socio-economic level. The paintings reveal that the city was inhabited by a rich elite, very close in terms of taste and status to the richest senators in Rome, to which Ostia is inextricably related.

Thanks to a collaboration between the CeSPRO, the *Istituto di Scienze del Patrimonio Culturale* (ISPC-CNR) and the *Université catholique de Louvain*, a large number of fragments could be analysed. The fragments were chosen according to their place of finding, distributed in different areas of the city, and their chronology (2nd century BCE – 1st century CE). Four contexts were selected: the *Caseggiato dei Lottatori*, the *Caseggiato delle Taberne Finestrate* and an unnamed building identified as V, II, 2 and a group of fragments of unknown origin, found in the archaeological deposit of the *Insula di Bacco Fanciullo*. The objectives of the analyses were the characterization of the materials and of the execution technique. The archaeometric approach may support, through the comparison of technological features of different groups of fragments, the attribution made by scholars, based on stylistic and archaeological perspective, to a specific period or a different workshop.

Nowadays, a high number of techniques are available for the analysis of wall paintings [14] starting from those non-invasive, portable, for *in situ* use, up to laboratory techniques conducted on the synchrotron lines of big facilities dedicated to cultural heritage [15].

Roman wall paintings and their constituent materials have been studied for several years [16] but still represent an interesting field of study. The topic is very vast, both in geographical and temporal terms and the knowledge of materials and techniques is not yet complete. In the last twenty years the Roman paintings have been studied not only by analysing samples taken through laboratory techniques [17–26], but increasingly favouring a multidisciplinary approach, with particular attention to non-invasive techniques [27–34].

The planning of the analytical protocol has to be based on different aspects such as the type of research questions (composition/fabrication condition), the type of material (extensive or limited possibilities of collecting samples) and the available resources (time, *in-situ*/*ex-situ* availability, budget).

Based on this context, the contribution of conservation scientists should be focused to the acquisition of the highest number and most significant chemical, molecular and structural information, in order to provide a comprehensive knowledge of the materials composition.

The most common approach when fragments are available consists on the sampling of a part of it for cross sectional analysis; this conventional survey is intrinsically weak since painted surfaces are highly heterogenous and the sample devoted to cross sectional analysis could not be fully representative of the actual situation. Instead of providing an overview of the paintings, an extremely detailed investigation of a randomly selected part of it is generated, depriving the scientific analyses of their outstanding and unique contribution to the historical, artistic, archaeological and conservation knowledge of the objects.

To address this critical issue, here an optimized analytical approach is proposed for the in depth study of the Ostia Antica painted fragments. The first step was based on non-invasive analyses of fragments with portable non-invasive techniques and, once acquired and evaluated the data, a second step is planned based on the collection of few microsamples from the fragments to be analysed with micro-destructive techniques.

The reasons why a preliminary non-invasive step was included in the protocol, instead of directly analysing cross sections, are: i) the need to analyse, on the same fragment, large areas (with imaging techniques) or different points (with single spot techniques), thus obtaining a general overview of the materials present; ii) the need to address the sampling to the more significant and complex areas, obtaining their detailed characterization and also reducing the size and number of samples; iii) the need to optimize the non-invasive analytical protocol on fragments, essential for the expected *in situ* measurement campaigns that will be planned in the framework of the collaboration with CeSPRO, where no longer fragments but paintings still in their original location will be anal-

ysed and compared with the data acquired in the actual non-invasive survey.

## 2. Materials and methods

The fragments were stylistically dated from the beginning of the 2nd century BCE to the end of the 1st century CE. They belong, as already mentioned, to four different contexts from Ostia Antica.

Fragments representative of each context were selected, favouring those containing more colours with the aim to study all the pigments used. Among hundreds of fragments, 28 were chosen for archaeometric studies as shown in Table 1, where the indication of the acronym and numbering is reported.

### 2.1. Analytical protocol - step 1

In the first step, non-invasive analyses have been performed starting from the imaging techniques such as UV induced Luminescence (UVL) to highlight and locate organic materials (colorants, binders or restoration materials) eventually present [35–38] and Visible Induced Luminescence (VIL), a very powerful tool to map the presence of a specific pigment, Egyptian blue [37,39–41].

For the photographic UVL a digital camera Canon EOS 7D (18 Mpixel, CMOS sensor) was used. The camera was equipped with Canon lens EFS 28 mm f/3.5 with B + W486 UV/IR blocking filter to cut reflected ultraviolet. As sources, two Flash Quantum T5D with B + W UV black 403 filters were used. The same set-up was used for acquiring visible images removing the filter from the flashes. For VIL acquisitions, the fragments were irradiated with visible light by using two flashes Quantum T5D mounted with B + W486 UV/IR; the infrared luminescence was collected with a modified (built–in filter for IR removed) Canon EOS 400D (10.1 Mpixel, CMOS sensor) with Canon lens EFS 28 mm with B + W 093 Infrared 830 blocking filter to cut all stray radiation from visible spectrum and thus collecting only infrared luminescence. A white Spectralon® plate (WS-1S-L Labsphere certified standard) was used as reference.

Fibre Optic Reflectance Spectroscopy (FORS) in UV–VIS-NIR range is a fast, non-invasive technique widely employed for pigments identification [42–45]. FORS spectra in 390–900 nm range, were acquired by using a Tungsten source (Ocean Optics mod. HL200) and a spectrometer (Ocean Optics mod. HR2000) equipped with optical fibres. The measuring head with 45° illumination and 0° signal collection allowed the acquisition of the reflectance spectrum of an area of about 2 $mm^2$. Each acquired spectrum was the average of 30 scans. As a reference, a Spectralon© plate (WS-1S-L Labsphere certified standard, 99% reflective material) was used. The acquired reflectance spectra were compared with reference one included in both ISPC-CNR spectral database (not published) and IFAC-CNR FORS spectral databases of pigments [46].

X-Ray Fluorescence (XRF) is a powerful technique for acquiring information about elemental composition of materials [47–49]. XRF spectra were collected by means of handheld Tracer III SD Bruker spectrometer, equipped with rhodium anode and solid state silicon detector energy dispersion system. The used set-up was: 40 keV and 12μA for 120 sec. The measuring area was an elliptical spot of 4 mm × 7 mm. For data elaboration ARTAX software was used after normalizing spectra to the intensity of Rh Kα at 20.21 keV.

Being both FORS and XRF non-invasive techniques, it was possible to acquire, for each fragment, several spectra in different coloured areas but also to repeat the measurements in areas of the same colour but on different spots. As far as possible, efforts have been made to perform the measurements on the same spot with the two techniques (XRF and FORS) also taking into account that the dimensions of their investigated areas are different. Moreover, it must be taken into account the FORS spectra may be influenced by the surface morphology and by the presence of underneath coloured layers, while to the XRF data, almost all the layers present, including the preparation ones may contribute.

All the areas analysed were documented with a portable digital microscope with different magnification (Scalar DG-2A, optical zoom 25-200x, magnification @ 25x - area 13 mm × 8 mm).

In Fig. 1 is reported, as an example, the image of a fragment with the indication of the analysed areas and documented with microphotos acquired with the digital microscope.

### 2.2. Analytical protocol - step 2

As already mentioned, based on the results of the first step, samples were taken from selected fragments. Sampling was done to obtain stratigraphic and morphological information not otherwise obtainable. Once the micro-samples were withdrawn, they were observed and documented under the microscope, and subsequently, thin and cross sections were obtained embedding the sample in epoxy resin (Epofix). In general, cross sections [50] were used for studying pigments by observing them with the optical microscope in reflected light under different magnifications according to the available microscopy objectives. In this case a Nikon Eclipse E600 optical microscope was used.

Oriented thin sections (30 μm thick) of plasters were observed in transmitted light with a ZEISS Axioscope A1 microscope at different magnifications. The image analysis software Axiovision was used for the morphological and morphometric observation, for the evaluation of binder/aggregate ratio.

In case of plasters, the petrographic approach permits accurate characterization of binder, aggregate and their ratio, the identification of composition, shape and grain size of aggregate, the assessment of presence of material providing hydraulicity and the evaluation of macroporosity. In addition, it is also possible to evaluate the number, thickness and cohesion of each layer [51–58]. Moreover, some suggestions on technology used for the preparation of mixtures and application of painting layers may be obtained.

Furthermore, both thin and cross sections were observed by using SEM and analysed with EDS. The instrument used was a SEM ZEISS EVO MA15 equipped with EDS and software OXFORD INCA 250 operating in both high vacuum condition (1.8 10–3 Pa; coated samples) and low vacuum (100 Pa; uncoated samples), 15 kV accelerating voltage, 700 pA emission current, working distance 9.5 mm.

Raman microscopy is a technique of choice for characterisation of surface layers of paints in art and archaeology for its high chemical specificity and lateral resolution. Measurements were carried out using a Senterra dispersive Raman microscope (Bruker Optik GmbH) equipped with a Peltier cooled CCD detector (1024 × 256 pixels). The laser excitation wavelength was 785 nm, 1200 grooves/mm grating and acquisition time ranging from 60 to 240 s. The microscope objectives used are 50x and 100x, with a lateral resolution of about 1 and 3 μm, respectively.

Lastly, in some cases, small parts of the sample withdrawn were separated under the microscope and analysed with Fourier Transform Infrared spectroscopy (FT-IR). FT-IR analyses were conducted with the ATR (Attenuated Total Reflectance) configuration. The instrument used was Alpha Bruker and each spectrum was the mean of 128 scans @ 4 $cm^{-1}$ resolution.

## 3. Results and discussion

The results of the two analytical steps will be reported and discussed together in the next paragraphs.

**Table 1**
Fragments under study with the acronym and numbering. The assigments to style and dating was based on stylistical analyses done by archeologists.

| ***Building/Wall/Style*** | ***Acronym and fragments*** | |
|---|---|---|
| *Caseggiato delle Taberne Finestrate*<br>Wall I<br>4th style<br>2nd half 1st c. AD | PI_A | 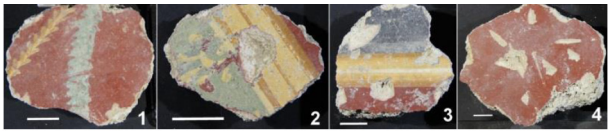 |
| | PI_B | 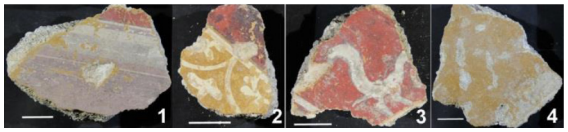 |
| | PI_C | 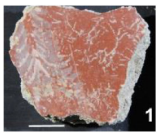 |
| *Caseggiato delle Taberne Finestrate*<br>Wall III<br>2nd style, 1st c. BC | PIII_A | 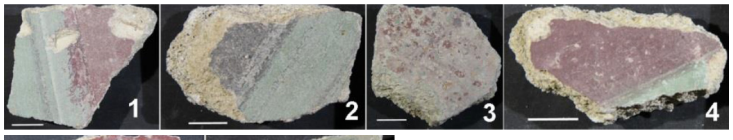 |
| *Caseggiato delle Taberne Finestrate*<br>1st style<br>end 2nd c. BC | PIII_B | 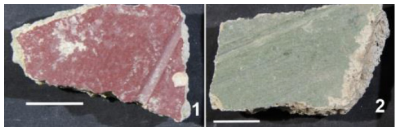 |
| *Caseggiato dei Lottatori*<br>Wall IV<br>4th style<br>2nd half 1st c. AD | PIV | 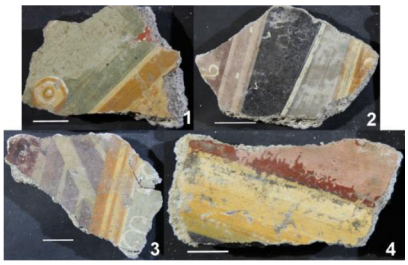 |
| *Deposit of Insula di Bacco Fanciullo*<br>4th style<br>2nd half 1st c. AD | PIV | 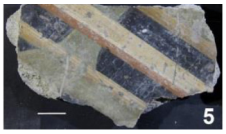 |
| *Caseggiato delle Taberne Finestrate*<br>Ceiling<br>4th style<br>2nd half 1st c. AD | SII | 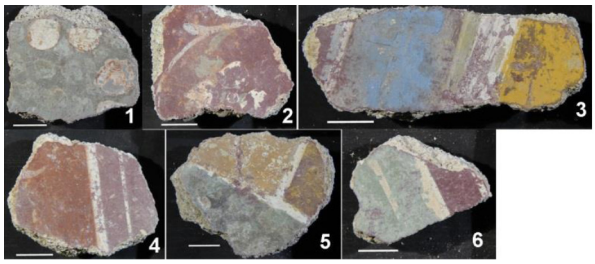 |
| *Caseggiato dei Lottatori*<br>4th style<br>2nd half 1st c. AD | PAV1 | 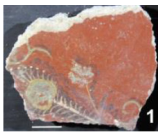 |
| *Building V,II, 2*<br>4th style<br>2nd half 1st c. AD | PAV2 | 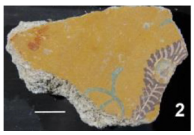 |

Images of UV induced Luminescence (UVL) of the 28 fragments did not highlight any peculiar emission. From this evidence, we can assume that there are neither organic pigments (e.g. lakes) nor pigments applied *a secco* (at least with binder characterized by an intrinsic fluorescence emission). On the contrary, weak signals of an organic material were found by FT-IR analysis. In particular, in two samples belonging to the PIV group where signals of an acrylic resin (most likely Paraloid B72) used in recent restoration, were found.

XRF technique detected, apart from the elements characteristic of each colour, discussed afterward, high counts of calcium (Ca) together with variable amounts of strontium (Sr). Calcium signal was expected since calcium-based materials are used as preparatory layers, binder or mixed with pigments to obtain different hues. Moreover, due to the penetration of XRF, contributions of carbonate materials from inner layers are expected. As far as strontium is concerned, this is an element also found in other contexts

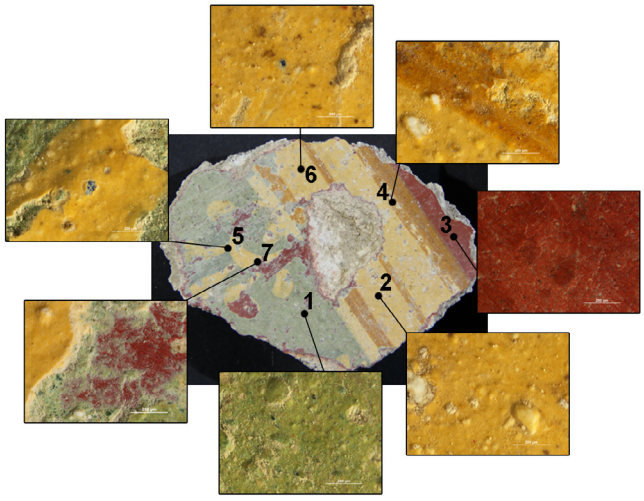


**Fig. 1.** Fragment PI_A2 with the indication of the areas analysed with non-invasive techniques (FORS and XRF) along with the microphotos acquired with the digital microscope (25X, bar 200 μm).

[29,31,59], generally associated with calcium compounds, since it is one of the calcium chemical substitute (cfr. Tab. S1).

### 3.1. Pigments

#### 3.1.1. White, grey and black colours

The white colour was mainly used for drawing the lines or the decorations. In most cases, calcite and dolomite pigments were used ($CaCO_3$ and $CaMg(CO_3)_2$, respectively), as indicated by the symmetric stretching modes of carbonates at 1087 $cm^{-1}$ (calcite) and 1098 $cm^{-1}$ (dolomite). The latter dolomite band represents a shoulder of calcite band, which is the main phase.

The greyish white-blue colour is obtained mixing a white and Egyptian blue pigments, validated by the results of the Micro-Raman spectroscopy and VIL investigations, respectively.

The black colour was due to carbon-based pigments that were not detected neither by XRF nor by FORS. Micro-Raman spectroscopy is effective for the detection of these black pigments and despite the strong photon absorption and fluorescence, the most characteristic D and G bands around 1350 $cm^{-1}$ and 1580 $cm^{-1}$ have been detected which unequivocally permit the identification of carbon black (Fig. S1a).

#### 3.1.2. Yellow colours

Yellow ochres were frequently used in Roman wall paintings [60,61]. This pigment was found in several fragments under study. It was used either for painting the first layer in contact with plaster or for the decorations on top of other colours, but also for imparting colour to the preparation layer in some fragments (PI_B1, PI_B2, see Fig. 4). The yellow areas analysed, ranging from light yellow to orange, were 29. All the FORS spectra acquired presented the characteristic features of iron-based pigments (absorption bands at about 400–500 nm, ~ 650 nm and ~900 nm) [44,62]. The spectra presented different reflectance values and a shift of the inflection point depending on the hue, (555 nm for yellow and 570 nm for orange hues, respectively). In Fig. 2a representative spectra are reported.

The XRF spectra acquired in all the yellow/orange areas were characterized by high counts of iron (Fe). The amount was variable also because yellow layers were sometimes superimposed to red ones also containing iron.

The FT-IR ATR analysis of a micro-sample taken from the fragment PI_B4 provided the identification of goethite mineral (α-FeO(OH)). This latter, which is the chromophore mineral in yellow ochre, exhibits its characteristic bands at 905 and 795 $cm^{-1}$ [63,64]. Furthermore, Raman spectroscopy confirmed the use of goethite in the yellow layers and hematite in the red ones, as demonstrated by their intense bands in the 200–600 $cm^{-1}$ range (Fig. 2b). Interestingly, hematite has been also used in the shades of the yellow areas, which have been spread using a mixture of yellow and red and dark red particles, as demonstrated by Raman spectroscopy (Fig.S1b and c). Tiny black particles of carbon black have been also detected; however, their presence is rare and it cannot be responsible for the dark hue of these areas.

#### 3.1.3. Red colours

Red is one of the most used colour in Roman wall paintings, which can be obtained either by inorganic minerals (cinnabar (mercury sulphide), realgar (arsenic sulphide) and iron oxide (hematite, red ochres)) or by synthetic compounds such as red lead (lead tetraoxide) [65]. Some papers concerning the composition of Roman wall paintings report red ochre as the only red pigment found [66–69] whereas in other literature case studies, both red ochre and cinnabar were identified in different areas [31,70]. In other cases, beyond "pure" red layers of both red ochre and cinnabar, admixtures of the two were also found [30,71].

In the fragments from Ostia, three different red hues were identified that can be described as follows: red-type1 - red colour, little bit dull; red-type2 - a more violet hue compared to red-type1; red-type3: a brilliant red with some black areas. The features in the FORS spectra allowed the identification of the three different pigments for which representative spectra are reported in Fig. 3a.

In red-type1 and red-type2 the FORS spectra showed the characteristic bands centered around 860–870 nm, typical of hematite [44,62]. The two red hues differ in an average lower reflectance for the red-type2, but the inflection point is very similar (590 ± 3 nm for red-type1 group and 593 ± 3 nm for red-type2 group) and close to that of the reference red ochre (590 nm). FT-IR spectra of two samples, belonging to red-type1 and red-type2 groups, confirmed the presence of hematite through to its characteristic bands around 535 and 470 $cm^{-1}$ [72].

XRF confirmed the presence of iron (Fe) as key element in all the spectra of the two groups. No differences were found in terms of other elements, such as manganese (Mn), which could have been responsible for the different hue for the red-type2 group. Therefore, the difference could be due to other factors than chemical composition such as the admixture with black pigments (carbon- or iron-based) [31] or to the particle size distribution as reported by Marshall et al. [73] or to a combination of the two. To clarify this question, Raman spectroscopy was performed on cross sections of samples with the two different reds (type1 and type2). In both cases hematite was identified; however, dark crystals in the red matrix of the red-type2 group have been observed, still made by hematite. These results indicate that two different kinds of hematite sources can be inferred: a fine powder used for the red matrix and coarse crystals for the dark particles, added with the intention of providing a violet hue to the paint layer.

The third group (red-type3) presents a completely different spectral shape of the FORS spectra compared to the previous two groups (Fig. 3a). The sigmoidal shape, with steep rise around the inflection point, is typical of semiconductors (realgar, minium and cinnabar) [44]. The inflection point, centered at 600 nm, points to cinnabar (HgS). The XRF spectra of all areas belonging to red-type3 group present the signals of mercury (Hg) and sulphur (S), thus confirming the identification of cinnabar (Fig. 3b). Moreover, in XRF spectra also significant signals of iron (Fe) were present. The presence of iron-based compounds was also suggested by weak signals observed in the FORS spectra (750–800 nm). Relying only on these data, it was not possible to determine if the iron-

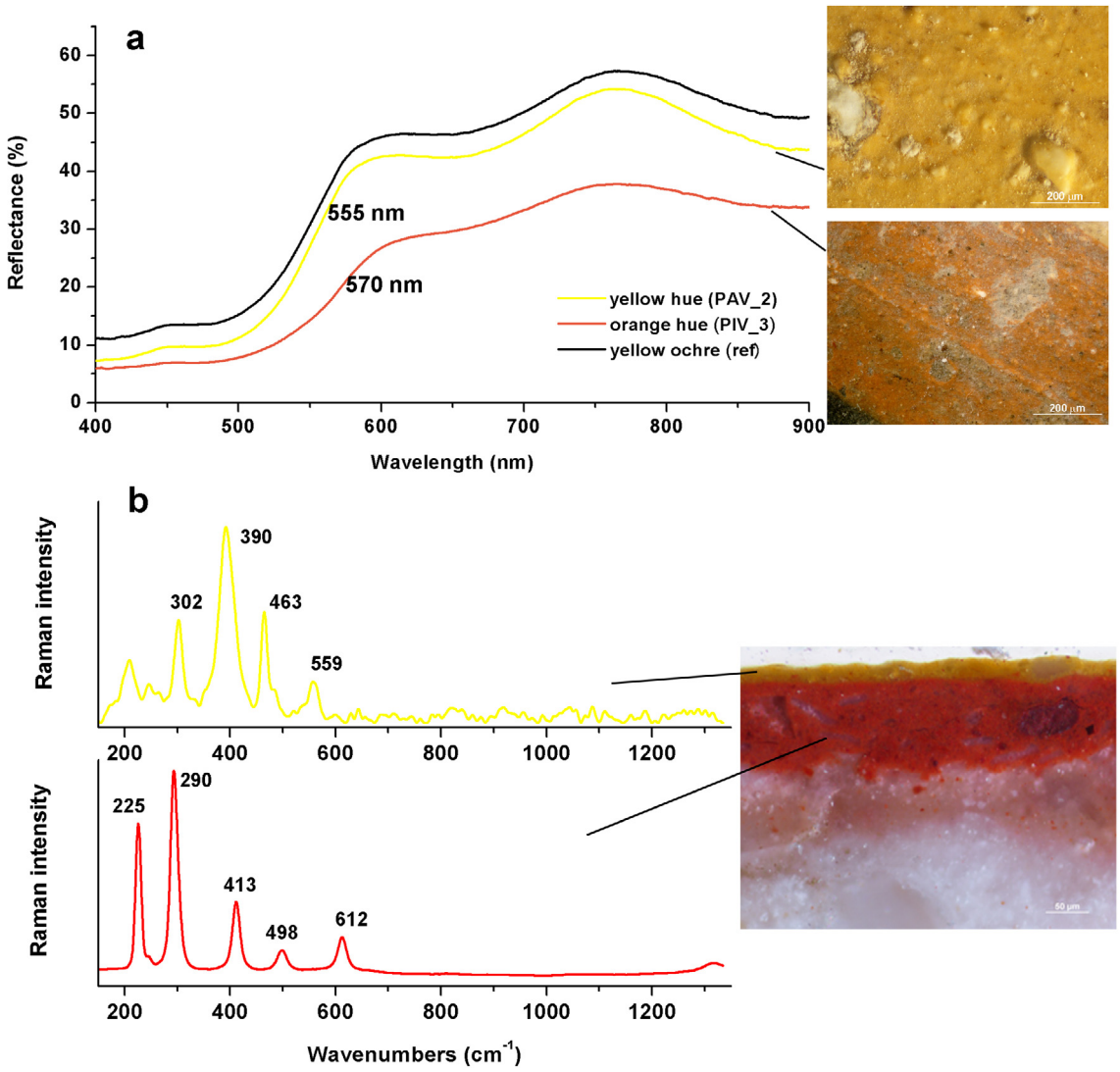


**Fig. 2.** a) FORS spectra of yellow hue (PI_A2 fragment) and orange hue (PIV_5 fragment) areas along with the microphotos acquired with the digital microscope of the same areas (25x; bar 200 µm) and reference spectrum of yellow ochre (ref); b) Raman spectra acquired on the cross section (20X; bar 50 µm) obtained from the sample taken from PI_A2 on the yellow layer (goethite) and red one (hematite).

based compound was mixed with cinnabar in the painting layer since a yellow iron-based preparation layer was present underneath the red external one (Fig. 4d).

The determination of the provenance of cinnabar could be of great importance and may give information about trade routes. During Roman period, localities from which cinnabar was supplied were the Roman province *Hispania Baetica* (probably corresponding to Almadén in Spain), Ephesus and Cyprus. No references exist for other quarries, such as those of Monte Amiata (Italy). The cinnabar from Almadén contains quartz while the one from Italy contains calcite and dolomite. These latter minerals could be present in very low amounts depending on the process of purification, and therefore are not conclusive for pigment provenance. Other elements, such as arsenic (As), is reported to be an indicator of the provenance from Monte Amiata [74]. The provenance of cinnabar has also been inferred by analysing the isotopes of sulphur [75] or lead (present as impurities) [76] and in both cases the data pointed to Spanish cinnabar. For the Ostia fragments it was only possible to underline the absence in the XRF spectra of the arsenic signals and of dolomite bands in the samples analysed by FT-IR, after which no hypothesis about provenance were possible.

Furthermore, in the red-type3 group a unhomogeneous blackening, more evident in the fragment PI_B2, was observed. In the red/black areas (Fig. 4a and Fig. 4b) the FORS spectra maintained almost the sigmoidal shape characteristic of cinnabar, while the reflectance was strongly reduced on blackened areas. In addition, the XRF spectra acquired on both red and black areas, showed no differences in terms of detected elements.

Blackening of cinnabar is a widespread phenomenon [34] described already in antiquity by Pliny the Elder and Vitruvius [77]. Some scholars made the hypothesis of the transformation of cinnabar to metacinnabar (black form) but without any analytical confirmation [78,79]. Further studies are related to panel paintings [80–82] and Roman wall paintings [83]. Various mechanisms of red α-HgS degradation have been proposed, but the issue is still under discussion. However, scholars agree that exposure to light and contact with halogens are the main factors influencing the degradation [77,84].

In the case of the fragments from Ostia, through the XRF spectra, the presence of chlorine (Cl) was detected, in respect to the mean counts (mean value of 22,500 ± 2,620 net counts obtained from 68 spectra) in significative amount in a few areas (PI_A2,

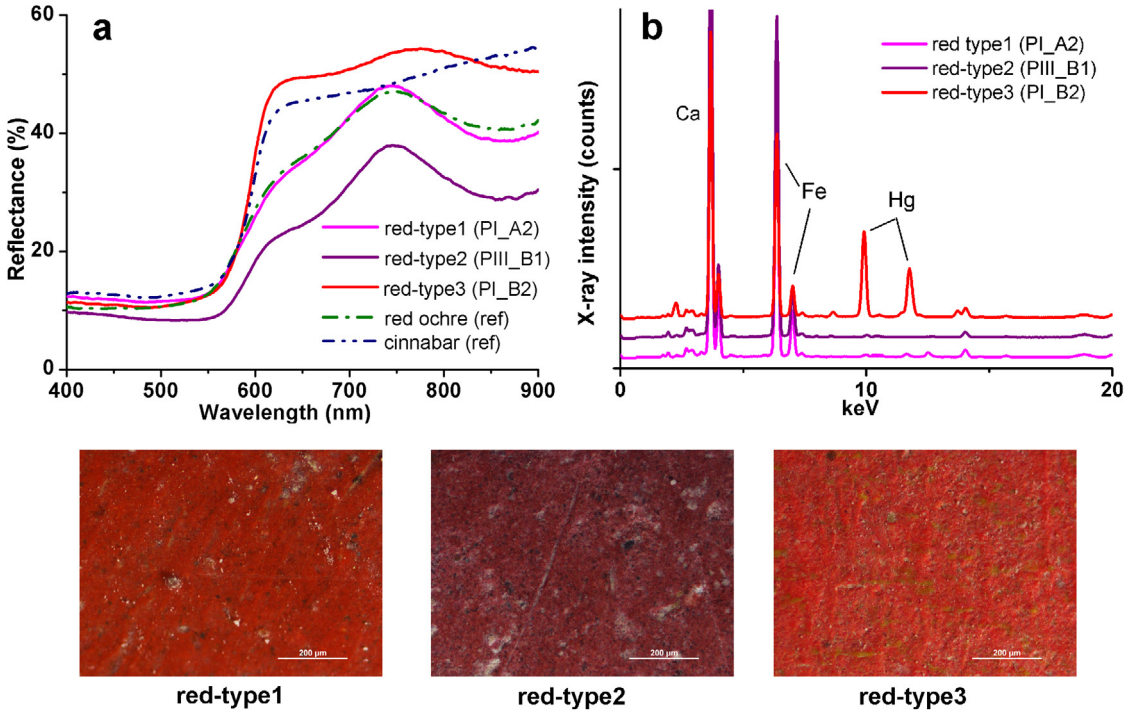


**Fig. 3.** FORS (a) and XRF (b) spectra of red-type1 (PI_A2 fragment), red-type2 (PIII_B1 fragment), red-type3 (PI_B2 fragment) along with the microphotos acquired with the digital microscope of the measured areas (25x; bar 200 μm).

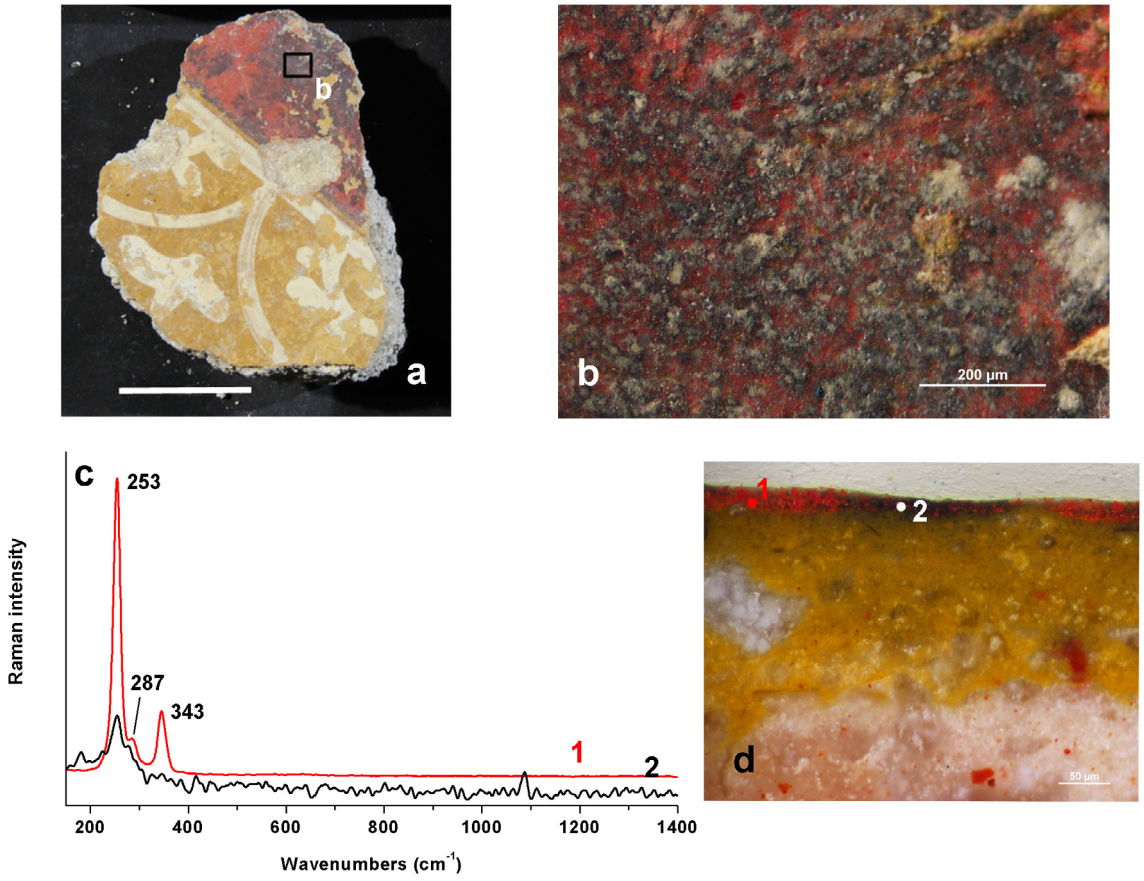


**Fig. 4.** (a) fragment PI_B2; (b) microphoto (25x; bar 200 μm) acquired with digital microscope corresponding to the black square on fragment PI_B2; (c) Raman spectra acquired on red and black crystals in the upper layer of cross section (20X, bar 50 μm) of a sample from fragment PI_B2 (d). The yellow layer and red crystals below the upper layer are constituted by goethite and hematite, respectively (spectra not reported). (For interpretation of the references to colour in this figure legend, the reader is referred to the web version of this article.)

56,7007,000 net counts; PI_A4, 125,000 net counts; PI_B4, 178,000 net counts) but not in the areas painted with cinnabar whether darkened or not. The only indication is that, at least in some fragments, chlorides were present. This is not unexpected since Ostia Antica is close to the sea and potentially all painted surfaces or buried fragments could have interacted with chlorides.

Raman spectra acquired on red and black crystals in the upper layer of cross section of a sample from fragment PI_B2 (Fig. 4c and Fig. 4d) confirmed that red crystals were made of cinnabar, while in the black areas the overall spectral intensity strongly decreases, in line with expectations, and weaker signals of cinnabar, as well as calcite, were detected. No other compounds, that could be responsible of black colour, were found. Although metacinnabar should have a Raman pattern similar to that of cinnabar, a contribution of cinnabar in the spectra acquired in the black areas cannot be completely excluded, considering its high Raman scattering cross section. Therefore, in this case no substantial contributions to the understanding of the degradation mechanism could be offered. For sake of completeness, the yellow layer and red crystals below the upper layer are constituted by goethite and hematite, respectively (spectra not reported).

### 3.1.4. Green pigments

Green is a colour found in almost all Roman wall paintings [85]. Very common is the use of ferro-magnesian silicate minerals belonging to the mica group, such as celadonite and glauconite [30,69,71]. More rarely, is also reported the use of malachite $Cu_2(CO_3)(OH)_2$, found as raw material in Pompei [86] but, very frequently, due to the high costs of this pigment, in admixtures with green earths to strengthen the colour hue [31,87].

In Roman period, green earths sources were Italy (Monte Baldo, Verona) and Cyprus. The two differ from each other for the presence of chromium (present probably as chromite) in the pigment from Verona [72,88]. Green earths containing chromium were found in fragments from Oplonti (Naples) and from Vigna Barberini (Rome) [59] and in some rooms of the Domus Aurea in Rome [28,89].

FORS spectra acquired in the green areas of the 28 fragments (25 areas) permitted the identification of green earth as main pigment used. FORS spectra were quite variable in terms of percentage of reflectance and shape and this can be due to either the presence of yellow or red layers below the green ones or to the presence of Egyptian blue mixed in all green areas in different amounts. In all the XRF spectra acquired on the same 25 green areas, the main signals were those of iron (Fe) together with potassium (K). The potassium counts were significantly higher (mean value green areas: 46.000300 ± 7.000 net counts) if compared to the other colours (mean value of yellow and red areas: 15.000 ± 5.000 net counts).

Moreover, the assignment of the different fragments to two distinct groups was done based on the presence of chromium signal in the XRF spectra (green-type1 with chromium and green-type2 without chromium). In Fig. 5 the net counts of chromium for each green area analysed are reported.

It was not possible to find a positive correlation between the iron and chromium counts as obtained by other authors [31] because in the XRF spectra, as already outlined, the underlying layers, made with iron-based pigments, also contributed to the total iron counts.

By observing the cross sections of the green layers under the SEM (Fig. 5c) it was possible to locate some small bright crystals (5–10 μm) showing the presence of chromium (Cr) and iron (Fe) by EDS analysis. The Raman spectra acquired in the same crystals (Fig. 5d), exhibit an intense band at 727 $cm^{-1}$ and a weak and broad peak around 550 $cm^{-1}$. As reported from literature [90], Raman frequencies of chromites ($FeCr_2O_4$) change as a function of the $Cr_2O_3$ content: the less is the $Cr_2O_3$ content, the higher is the frequency. In the quoted paper [90] a list of 33 chromites is reported in order of decreasing $Cr_2O_3$ content showing that the Raman band in the 600–800 $cm^{-1}$ range shifts from 685 $cm^{-1}$ to 738 $cm^{-1}$. Therefore, the selected crystals analysed are ascribable to a chromite with low $Cr_2O_3$ content. In a few spectra, bands related to organic compounds were also detected.

FT-IR spectra were acquired on seven green microsamples, and the quite well resolved bands suggested the presence of celadonite in all samples. In the FT-IR spectrum reported as an example in Fig. 6, three bands at 3601, 3555, 3534 $cm^{-1}$ are characteristic of the hydroxyl. Other bands positioned 1075, 975, 956 $cm^{-1}$ (Si-O stretching), 799, 681 $cm^{-1}$ (R-O bending) and 494, 460, 440 $cm^{-1}$ (Si-O-R and R-O-H bending) are linked to celadonite [91–95].

In addition to the signals of celadonite, also the main bands of calcite ($CaCO_3$) at 1453, 875 and 712 $cm^{-1}$ were evident together with those of aragonite, present in variable amount, a polymorph of calcite with characteristic signal at 855 $cm^{-1}$ (Fig. 6). Aragonite was usually associated with the more precious pigments. Some scholars report the presence of aragonite in some samples from Reggio Emilia (IT) dated to 1st century AC [78]. According to Mazzocchin [96], in northern Italy, the use of white pigments containing calcite and aragonite has been observed since the Imperial Age. In fact, precious white pigments containing large amounts of aragonite were imported from Greece and Egypt, in this period [97]. Unfortunately, in the case of the fragments from Ostia, FT-IR analyses were conducted only on few samples therefore it was not possible to have a comprehensive evaluation on the presence/absence of aragonite in the different colours. From the data collected it is possible to state that aragonite was present only in the green (7 samples) while was absent either in yellow (2 samples) or red (2 samples) analyzed.

Moreover, in the XRF spectra signal of copper (Cu) was also present. These could be due to green copper pigments such as malachite which, however, would not have been identified through the non-invasive techniques used. Nevertheless, the presence of malachite was excluded on the basis of μ-Raman and FT-IR data. Copper could also be related to Egyptian blue mixed with green earth, a quite common practice of Roman artists [30,88,99,100] and which is also the one adopted in Ostia.

All the green areas, indeed, gave positive results to VIL survey. In Fig. 7 the images in visible light (a) and VIL (c) of fragment PIII_A1 are reported together with a microphoto of green layer, acquired with the digital microscope, where blue crystals are clearly visible (b). The bright luminescence in Fig. 7c highlights the presence of Egyptian blue.

### 3.1.5. Blue colours

The only blue pigment identified was Egyptian blue [101,102]. Through the VIL images it was possible to observe its distribution, even if present in small quantities [36–40]. As already described before, Egyptian blue pigment was used extensively in green areas mixed with green earth to enhance the brightness of green colour (Fig. 7). Moreover, the practice of mixing Egyptian blue to impart special hues to other colours was quite diffused in the fragments from Ostia, since Egyptian blue was also identified in yellow and grey areas (Fig. 8a-c). It was also used for specific decorations such as the peacock feathers of the fragment PAV_1 (Fig. 8d-f).

One fragment belonging to the PI_B group deserves special attention. In this group there are neither blue nor green backgrounds but in the fragment PI_B3 the VIL survey revealed the presence of Egyptian blue, clearly visible from the image in Fig. 9b. The presence of this pigment was also clearly visible in the microphotos acquired with optical microscope (Fig. 9c, Fig. 9d). The drawn lines containing Egyptian blue, which were not very evident in the image in visible light, did not follow the

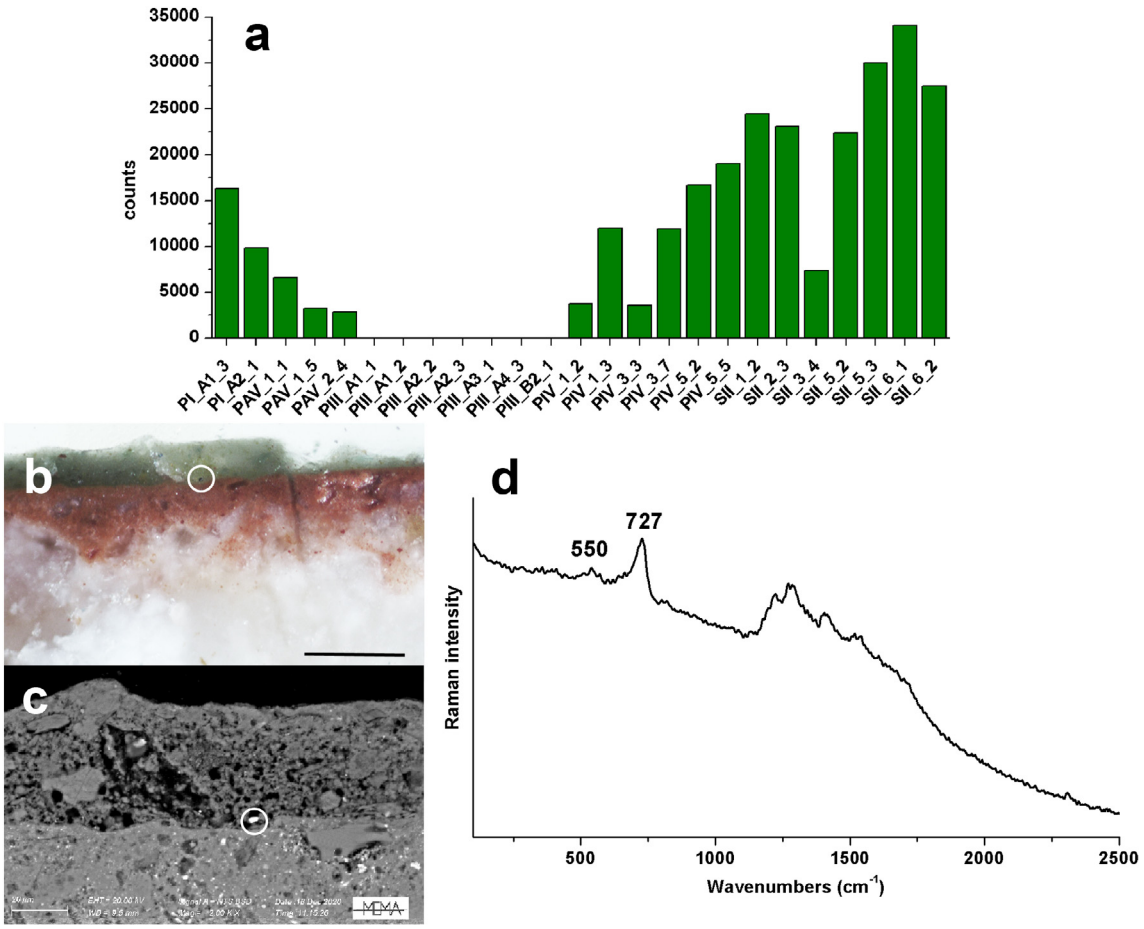


**Fig. 5.** (a) Counts of chromium in the XRF spectra of the green areas in the fragments. Cross section of sample taken from fragment PI_A2 under the optical microscope (b, bar 100 μm) and SEM backscattered image (c, bar 20 μm). (d) Raman spectrum of the crystal highlighted by the white circle in (b) and (c).

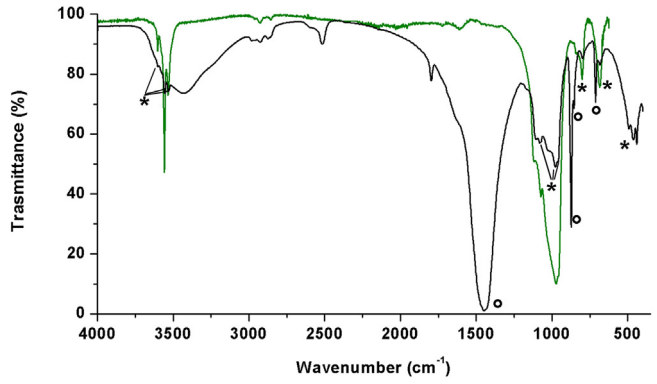


**Fig. 6.** FT-IR spectrum of a green sample (sampled from fragment PIII_A1) (black line) compared with the reference spectrum (green line) of celadonite from IRUG database (MP185) [98]. The asterisks pointed the bands characteristic of celadonite. The circles pointed the bands of calcite (1453, 875 and 712 $cm^{-1}$) and aragonite (1453, 855 $cm^{-1}$).

white colour decoration but overlapped and crossed it. The reason for this is not clear because the fragment was very limited in dimensions. It would be interesting to study other similar fragments to further clarify the role of these findings.

Notwithstanding the extensive use of Egyptian blue in almost all the fragments studied, the only blue area was present in fragment SII_3. The VIL image (Fig. 10b) showed a very bright luminescence indicating the presence of Egyptian blue (Fig. 10c) confirmed the use of this pigment.

### 3.2. Stratigraphic observations

The stratigraphic observations of some representative microsamples, performed with optical and electronic microscope, allowed to infer some evidences. The data allowed to highlight the correlation between different styles and the thickness of the painted layers, to characterize raw materials used for the plaster and to propose some hypotheses on the techniques of pigment application [55,71,103,104]. The plasters of Wall I, groups A, B and C, 4th style (Fig. 11a) are characterized by a painted layer with a variable thickness, ranging from 20 to 30 μm, applied with "*mezzo fresco*" technique, a slight interface between painted layer and background was observed (Fig. 11b). Under the painted layer, regardless of the colour on surface, a red zone, coloured by adding iron oxides to lime putty, with irregular thickness, spread in the first millimeters of the preparation layer, was observed. The preparation layer has a mean thickness of 45 mm and was realized by mixing calcic lime with crushed carbonate rock fragments (travertine) having sub-angular shape and grain size ranging from 1 mm to 100 μm. The aggregate has a heterogeneous distribution in the mixture, indeed in the final portion of layer only fractured lime is present. The mean ratio binder/aggregate is 1/2 (Fig. 11c). Under this layer a plaster made by mixing calcic lime with sub angular grains of volcanic rocks (*pozzolana*), carbonate rocks fragments (travertine and micritic limestone) and pyroxenes is present

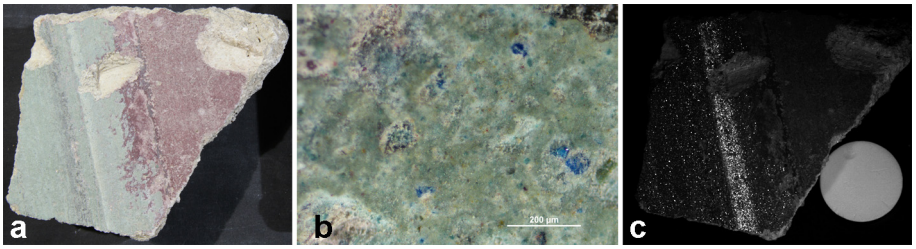


**Fig. 7.** Fragment PIII_A1 - (a) visible light, (c) VIL image, (b) microphoto (25x, bar 200 µm) of the green layer with some blue crystals of Egyptian blue.

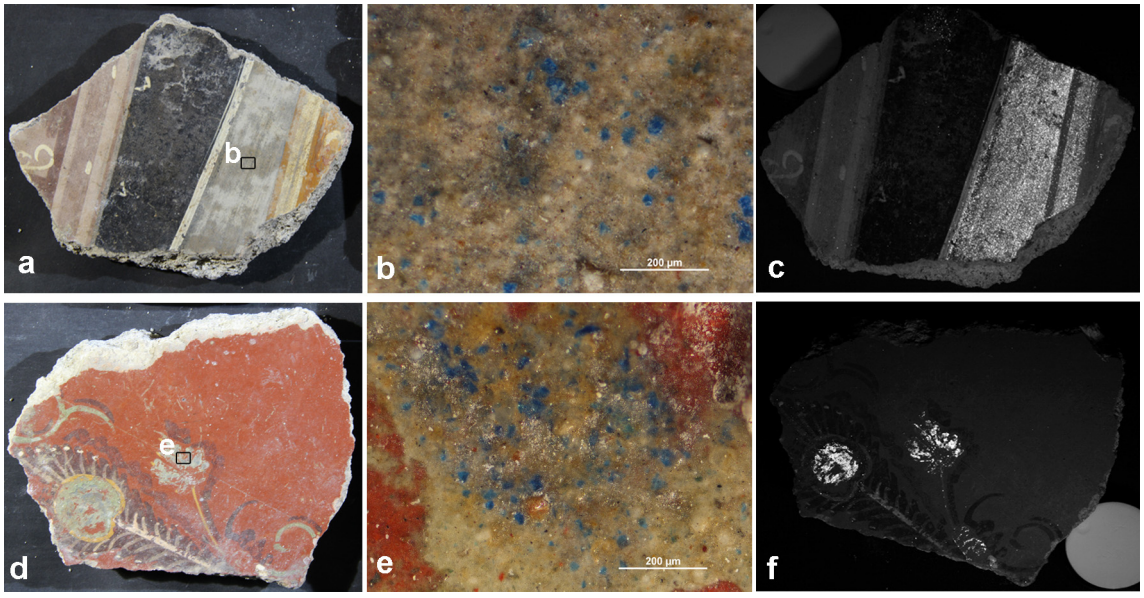


**Fig. 8.** Fragments PIV_2 (a) and PAV1 (d) with the corresponding VIL images (c, f) and microphotos acquired digital microscope of areas indicated by black squares (b, e, 25X, bar 200 µm).

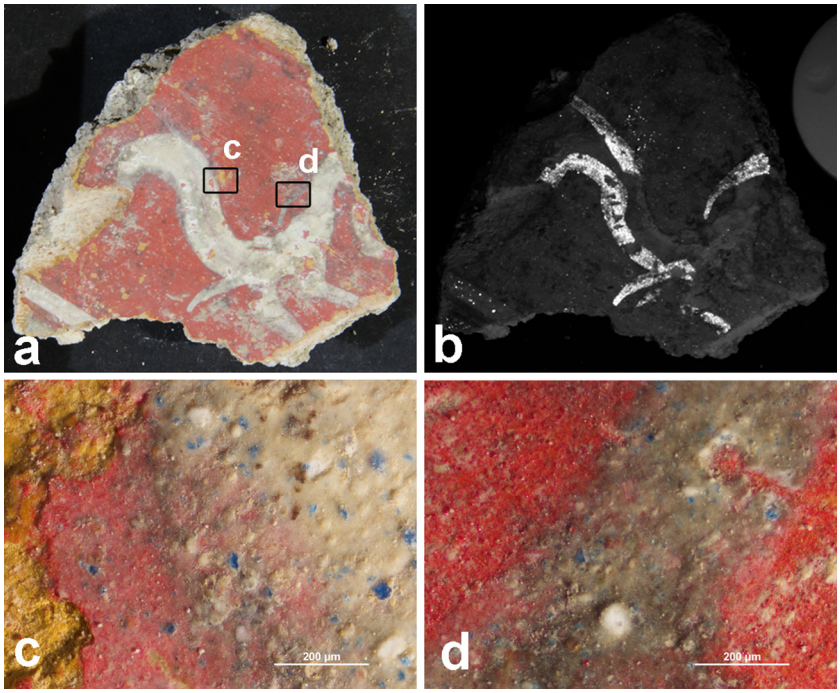


**Fig. 9.** VIS and VIL images of fragments PI_B3 (a) and (b) and (c, d) microphotos (25X, bar 200 µm) acquired with digital microscope of areas indicated by black squares in (a).

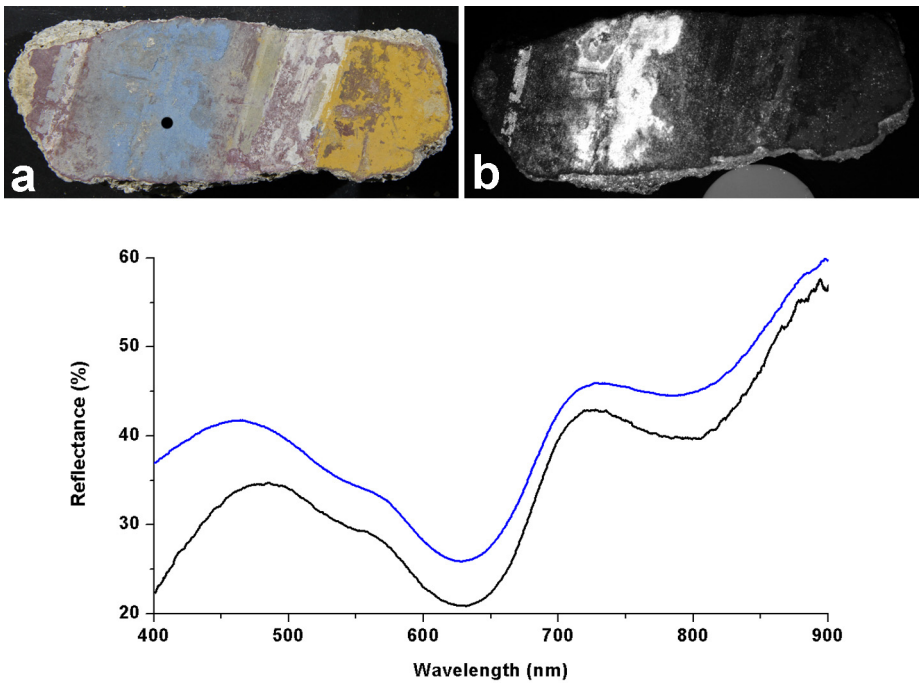


**Fig. 10.** VIS and VIL images of fragments SII_3 (a) and (b) and FORS spectrum (black line) acquired on the fragment (black dot in (a)) compared with FORS reference spectrum of Egyptian blue (blue line).

(Fig. 11d). The ratio binder/aggregate is about 1/3 for all the samples, and the grains of aggregate are well distributed in the mixture. Their grain size ranges from 1 to 1.5 mm to 100 μm. A scarce macroporosity, due to microcracks, was observed.

The samples of Wall III, groups A and B, belonging to 1st and 2nd style, exhibit a painted layer, rough and irregular, of thickness 30–50 μm, applied with "*a fresco*" technique on a typical *marmorino* layer. A continuity between layers was observed in cross section (Fig. 11e) and SEM (Fig. 11f) images.

The *marmorino* was obtained mixing calcic lime with calcite crystals (ratio binder/aggregate ranging from 1/3 to 1/4) (Fig. 11g). The calcite has a strong angular shape and a bimodal grain size distribution (main granulometric classes 1–2 mm and 100–150 μm). The underneath layer was obtained mixing calcic lime with volcanic rocks, single crystals of pyroxenes, fragments of carbonate rocks. The ratio binder/aggregate is about 1/3, the maximum grain size of 1–2 mm and the minimum of 200–300 μm.

The samples of Wall IV, 4th style, have a similar stratigraphic sequence with respect to those of wall I. A red coloured zone in the plaster, under the painted layer was also visible, except for the sample PIV_4. Some samples belonging to this wall show an abundant presence of lime lumps in the plaster layer referred to under-burnt fragments of limestones used for the preparation of the binder. In the aggregate of underneath plaster layer a prevalent presence of pyroxenes was evidenced (Fig. 11h). A more complex layering was observed for sample PIV_1, with the overlapping of new layers painted with "*a secco*" technique on previous "*a fresco*" layers. It was possible to observe 1) an external yellow layer (15–20 μm thick), 2) a first white layer (50 μm thick), 3) a second white layer (20 μm thick), 4) a red painted layer obtained with iron oxides finely dispersed in the lime putty. Breaks associated with 2–3 μm thick Ca-carbonate enriched level are clearly distinguishable at the interface between layers 4 and 3, layers 3 and 2 and layers 2 and 1 (Fig. 11i, Fig. 11l).

The samples coming from a ceiling decoration (samples SII) showed a painted layer with variable thickness, a second layer made of calcic lime added with travertine and calcite cristals, with subangular shape and with grain size ranging from 1.5 mm to 100 μm, a third layer obtained mixing lime with fragments of volcanic rocks, pyroxenes and carbonate rocks. The volcanic rock fragments have a maximum grain size up to 4 mm.

The PAV_1 sample presented similar characteristics with respect to plasters of Wall I and IV, while the PAV_2 sample has peculiar characteristics, different from all other samples, since, under the *marmorino* a plaster layer obtained mixing calcic lime with *cocciopesto* (crushed ceramic fragments) and volcanic fragments was observed.

As briefly described above, a peculiar aspect of the fragments belonging to 4th style is the presence of an intentional coloured zone, obtained by adding iron oxides (red or yellow) to lime putty, in the first millimeters of the preparation layer [105]. This kind of practice seems not to be applied for the fragments belonging either to 1st or 2nd style.

The coloured underlayers, specifically cinnabar on iron-based yellow, were found in wall paintings in other Roman sites in Europe such as England and France [106,107] and more recently in wall paintings from Solunto (1st century CE) [34], even if in these cases it is not specified if the yellow was due either to a paint layer or to a coloured plaster. A similar stratigraphy (cinnabar on yellow coloured plaster) was found in fragments of wall paintings from the archaeological site of Agios Donatos (GR) [108,109].

## 4. Conclusions

The optimized analytical approach proposed, based on two-step diagnostics, proved to be appropriate for the identification of pigments and the techniques employed for the realizations of the wall paintings (Table 2). The use of complementary non-invasive techniques allowed a preliminary analytical identification of painting materials, which is a fundamental step when dealing with hundreds of fragments. The micro-invasive stratigraphic analysis by SEM-EDS, μRaman spectroscopy and petrographic observations

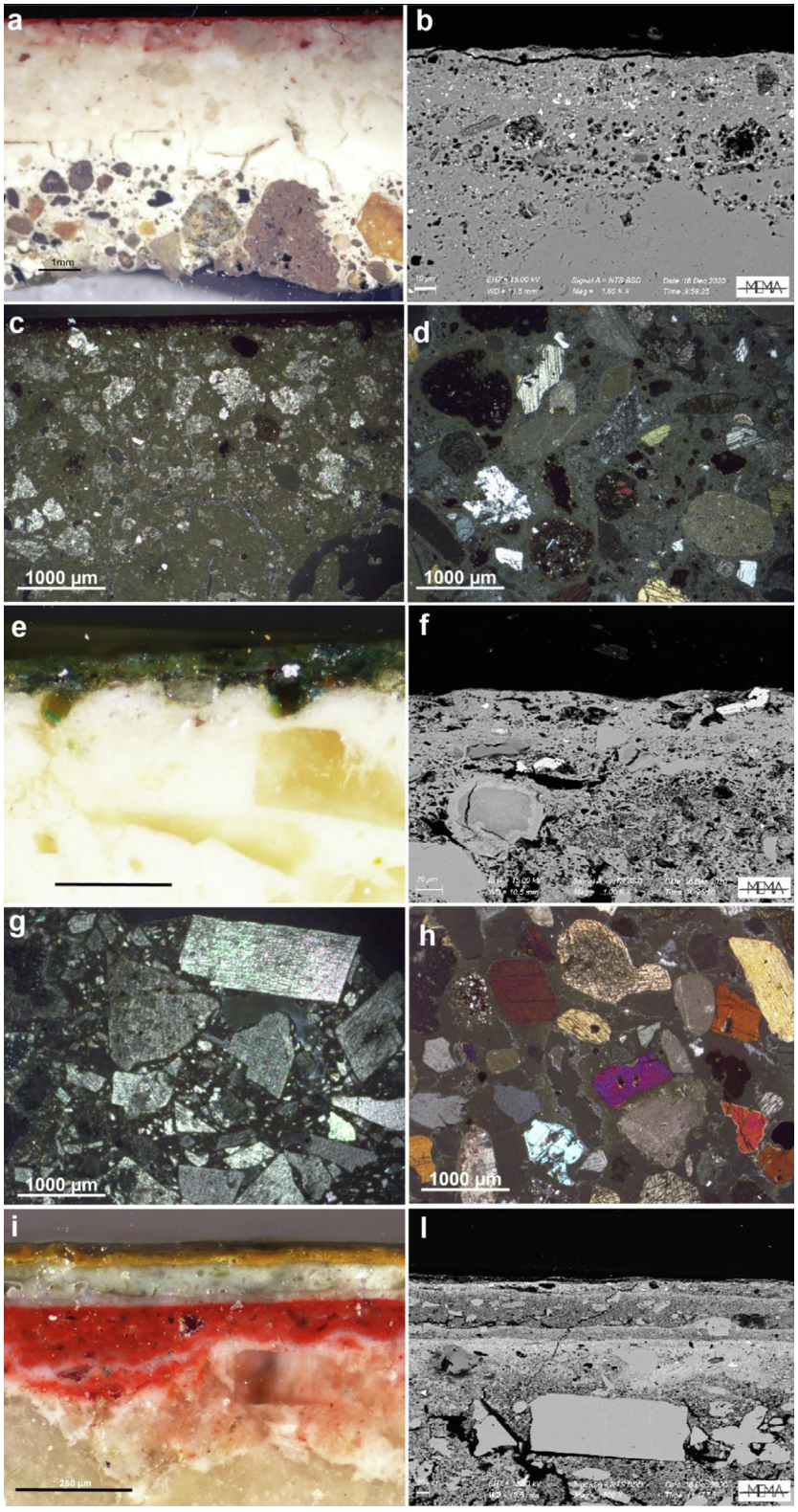


**Fig. 11.** Sample PI_A4 - (a) cross section (bar 1 µm), (b) BSE image of paint layer and red zone (bar 10 µm), (c) microphotograph of thin section under polarized microscope of the first plaster layer (crossed nicols, bar 1000 µm), (d) microphotograph of thin section under polarized microscope of the second plaster layer (crossed nicols; bar 1000 µm). Sample PIII_B2 - (e) cross section (bar 250 µm), (f) BSE image of paint layer (bar 20 µm), (g) microphotograph of thin section under polarized microscope of "marmorino" layer (crossed nicols; bar 1000 µm). Sample PIV_1 - (h) microphotograph of thin section under polarized microscope plaster layer with aggregate enriched in pyroxenes (crossed nicols; bar 1000 µm). PIV_1 - (i) (cross section, bar 250 µm) l) BSE image (bar 20 µm).

allowed to deepen the knowledge about specific features of the paint and preparation layers. The results demonstrated the use of a great richness of palette typical of Roman wall paintings, even with the use of more expensive pigments. For example, three different red pigments were identified even if there was not a strict correlation with the use for the different styles (red1 and red2

**Table 2**
Summary of the results obtained in the two steps protocol.

| Location and style | Groups (n. of fragments) | Pigments | | | Plaster | | |
|---|---|---|---|---|---|---|---|
| | | *colours* | | *painted layers* | *first layer* | | *second layer* |
| | | appearance | identification | thickness (cross section) | thickness | aggregate | aggregate[@] |
| Wall I 4th style 2nd half 1st c. AD | group A (4, A1-A4) | white black/grey yellow red green blue # | calcium based n.i. yellow ochre red ochre (type1) green earth (type1) Egyptian blue | yellow (20 μm) green (20 μm) red (100 μm) all colours on red preparation | 4–5 mm 80–100 μm red coloured | travertine 1 mm to 100 μm | *pozzolana* carbonate rock fragments pyroxenes |
| | group B (3, B1-B3) | white black/grey yellow red green blue # | calcium based n.i. yellow ochre cinnabar (type3) n.p. Egyptian blue | red (20 μm) on yellow preparation yellow (100 μm) on red preparation | 4–5 mm 80–100 μm red coloured | | |
| | group C (1, C1) | white black/grey yellow red green blue # | n.p. n.p. n.p. red ochre (type1) n.p Egyptian blue | red (100–200 μm) on red preparation | n.i. 200 μm red coloured | | |
| Wall III 2nd style 1st c. BC | group PIII_A (4, A1-A4) | white black/grey yellow red green blue # | calcium based n.i. yellow ochre red ochre (red2) green earth (type2) Egyptian blue | green/blue (30–50 μm) red (30 μm) | 7–10 mm | calcite (*marmorino*) 1–2 mm 100–150 μm | pyroxenes *pozzolana* carbonate rock fragments |
| 1st style end 2nd c. BC | group PIII_B (2, B1-B2) | white black/grey yellow red green blue # | n.p n.p n.p red ochre (type2) green earth (type2) Egyptian blue | green/blue (50 μm) | 7–10 mm | | |
| Wall IV 4th style 2nd half 1st c. AD | group PIV (4, 1–4) | white black/grey yellow red green blue # | calcium based n.i. yellow ochre red ochre (red1) red ochre (red2) green earth (type1) Egyptian blue | repainting on original red (50 μm) on red preparation | 5 mm 80–100 μm red coloured | travertine lime lumps | pyroxenes carbonate rock fragments *pozzolana* |
| 4th style 2nd half 1st c. AD | group PIV (1, 5) | white black/grey yellow red green blue # | n.p. n.i. n.p. n.p. green earth (type1) Egyptian blue | green (30 μm) on red preparation | 5 mm 1 mm red coloured | | |
| Ceiling 4th style 2nd half 1st c. AD | group SII (6, 1–6) | White black/grey yellow red green blue # blue § | calcium and lead based n.i. yellow ochre red ochre (red1) red ochre (red2) green earth (type1) Egyptian blue Egyptian blue | no cross sections | 2–3 mm | calcite and travertine 1.5 mm to 100 μm | volcanic and carbonate rock fragments pyroxenes |
| 4th style 2nd half 1st c. AD | PAV (1, 1) | white black/grey yellow red green blue # | calcium based n.i. yellow ochre red ochre (red1) green earth (type1) Egyptian blue | red (20–30 μm) on red preparation | 10 mm 500–800 μm red coloured | travertine 1 mm to 100 μm | *pozzolana* carbonate rock fragments pyroxenes |
| 4th style 2nd half 1st c. AD | PAV (1, 2) | white black/grey yellow red green blue # | calcium based n.i. yellow ochre red ochre (red1) green earth (type1) Egyptian blue | yellow (20–30 μm) on red preparation | n.d. 500–800 μm red coloured | calcite (*marmorino*) | *cocciopesto* pyroxenes |

n.i. – not identified; n.p.- not present; # present only in admixture with other pigments; § not mixed, present as blue area; [@]in order of abundance.

were identified in the same group). On the contrary, green earth containing chromite was found only in those fragments belonging to 4th style thus demonstrating a change in the supply of green earth.

Moreover, differences in the preparatory layer in term of both materials and techniques allowed to compare different groups and to confirm the stylistic attribution. It is interesting to see how style and technique are strongly related. Each period has its own characteristics: although technical differences between paintings of First Style (2nd c. BC) and Second Style (1st c. BC) are not very strong (PIII A and B), paintings of Fourth Style (1st c. AD; PI, PIV, SII and PAV) are completely different and easily distinguishable. Fourth Style fragments, especially PI (*Caseggiato delle Taberne Finestrate*) and PIV (*Caseggiato dei Lottatori*), share many similarities that could indicate the work of a same group of painters in different areas of the city. In particular, the coloration of plaster seems to be a practice exploited only in those contexts and it could be interpreted as a technical peculiarity of the Ostian painters of this period.

Thanks to the implementation of an educated multi-technique analytical approach, the materials and techniques could be fully revealed giving valuable information while minimising the sacrifice of precious original materials.

## CRediT authorship contribution statement

**Bracci Susanna:** Conceptualization, Investigation, Methodology, Data curation, Writing - original draft, Supervision. **Cantisani Emma:** Investigation, Methodology, Data curation, Writing - review & editing. **Conti Claudia:** Investigation, Methodology, Data curation, Writing - review & editing. **Magrini Donata:** Investigation, Methodology, Data curation, Writing - review & editing. **Vettori Silvia:** Investigation, Methodology, Data curation, Writing - review & editing. **Tomassini Paolo:** Resources, Writing - original draft. **Marano Martina:** Resources, Writing - original draft.

## Declaration of Competing Interest

The authors declare that they have no known competing financial interests or personal relationships that could have appeared to influence the work reported in this paper.

## Acknowledgments

The authors would like to thank Dr. Laura Chiarantini and Dr. Daniele Borrini (Centro Interdipartimentale di Microscopia Elettronica e Microanalisi MEMA of the University of Florence) for their help and support. Moreover, we are particularly thankful to the Parco archeologico di Ostia antica and specifically to Mariarosaria Barbera, Alessandro D'Alessio, Claudia Tempesta, Paola Germoni, Antonella Docci and Tiziana Sorgoni for their support.

## Funding

This research did not receive any specific grant from funding agencies in the public, commercial, or not-for-profit sectors.

## Appendix A. Supplementary material

Supplementary data to this article can be found online at https://doi.org/10.1016/j.saa.2021.120260.

## References

[1] C. Pavolini, Ostia, nuova edizione rivista e aggiornata, Guide Archeologiche Laterza, 11, Rome, 2018.
[2] J.-P. Descœudres, (Ed.), Ostia. Port et porte de la Rome antique, Catalogue d'exposition, Musée Rath de Genève, 23 février-22 juillet 2001, Geneva, 2001.
[3] S. Falzone, Ornata aedificia, Pitture parietali dalle case ostiensi, Istituto Poligrafico dello Stato, Rome, 2007.
[4] J. DeLaine, Housing in Roman Ostia, in: D.L. Balch, A. Weißenrieder (Eds.), Contested Spaces, Houses and Temples in Roman Antiquity and the New Testament, Tübingen, 2021, pp. 327–354.
[5] C. Conte, S. Falzone, P. Tomassini, Contesti di pittura inediti della tarda epoca repubblicana e della prima età imperiale, conservati nei Depositi di Ostia, in S. T.A.M. Mols, E.M. Moormann (Eds.), Context and meaning. Proceedings of the twelfth International Conference of the Association Internationale pour la Peinture Murale Antique, Athens, September 16-20, 2013, (BaBesch Supplements 31), Leuven-Paris-Bristol, 2017, 343-348.
[6] C. Conte, D. Dininno, S. Falzone, R. Lazzaro, P. Tomassini, Contesti di pittura frammentaria conservati nei Depositi Ostiensi: nuove testimonianze di soffitti di quarto stile, Forum Romanum Belgicum [online] 15, article 15.2, 2018, [http://www.bhir-ihbr.be]
[7] S. Falzone, 010, Luxuria privata. Edilizia abitativa e arredo decorativo a Ostia e a Roma in età tardo-repubblicana, in: A. Wallace Hadrill (Ed.), Proceedings of the XVIIth International Congress of Classical Archaeology - Rome, 22-26 Sept. 2008, Rome, 2010.
[8] S. Falzone S. Pittura parietale di Ostia (I secolo a.C./I secolo d.C.): i contesti domestici, in S.T.A.M. Mols, E.M. Moormann (Eds.), Context and meaning. Proceedings of the twelfth International Conference of the Association Internationale pour la Peinture Murale Antique, Athens, September 16-20, 2013, (BaBesch Supplements 31), Leuven-Paris-Bristol, 2017, 335-342.
[9] S. Falzone, Gli arredi decorativi delle domus ostiensi (I sec. a.C. – I sec. d.C.): progetto di studio delle pitture frammentarie conservate nei Depositi Ostiensi, in C. De Ruyt/T. Morard/F. Van Haeperen (eds.), Ostia antica : Nuovi studi e confronto delle ricerche nei quartieri occidentali, Actes du colloque international de Rome, 22-24 Septembre 2014, Rome-Bruxelles, 2018, 87-98.
[10] S. Falzone, Gioia C., Marano M., Tomassini P, Des enduits « de seconde main »: les peintures fragmentaires oubliées dans les dépôts de Rome et Ostie, in J. Boislève, A. Dardenay, F. Monier (Eds.), Peintures et stucs d'époque romaine. Études toichographologiques, actes du XXIXe Colloque de l'Association Française pour la Peinture Murale Antique (Pictor 7), Bordeaux-Pessac, (2018) 197-206.
[11] M. Marano, Affreschi di IV stile pompeiano provenienti dallo scavo del Caseggiato dei Lottatori ad Ostia (V, III, 1), in S.T.A.M. Mols, E.M. Moormann (Eds.), Context and meaning. Proceedings of the twelfth International Conference of the Association Internationale pour la Peinture Murale Antique, Athens, September 16-20, 2013, (BaBesch Supplements 31), Leuven-Paris-Bristol, 2017, 349-354.
[12] M. Marano, Rivestimenti pittorici di IV stile da Ostia: studio dei frammenti rinvenuti negli scavi del Caseggiato dei Lottatori, Forum Romanum Belgicum [online] 15, article 3, 2018, [http://www.bhir-ihbr.be].
[13] P. Tomassini, L'apporto delle decorazioni frammentarie del Caseggiato delle Taberne Finestrate per la conoscenza della pittura c.d, "pompeiana" ad Ostia, Scienze dell'Antichità 25 (2) (2019) 67–76.
[14] S. Bracci, G. Bartolozzi, Wall paintings - diagnostic and archeometric studies, in. L. Sabbatini, I. D. van der Werf (Eds.), Chemical Analysis in Cultural Heritage, De Gruyter, Berlin, 2020, 253-271. Doi: 10.1515/9783110457537-toc.
[15] R. Debastiani, R. Simon, D. Batchelor, G. Dellagustin, T. Baumbach, M. Fiederle, Synchrotron-based scanning micro-X-ray fluorescence applied to fragments of Roman mural paintings, Microchem. J. 126 (2016) 438–445.
[16] H. Davy, Some experiments and observations on the colours used in painting by ancient, Philos. Trans. R. Soc. London 105 (1815) 97–124.
[17] G.A. Mazzocchin, F. Agnoli, M. Salvadori, Analysis of Roman age wall paintings found in Pordenone, Trieste and Montegrotto, Talanta 64 (2004) 732–741.
[18] J.S.E. Villar, H.G.M. Edwards, An extensive colour palette in Roman villas in Burgos, Northern Spain: a Raman spectroscopic analysis, Anal. Bioanal. Chem. 382 (2005) 283–289, https://doi.org/10.1007/s00216-004-2876-7.
[19] A. Duran, M.C. Jimenez De Haro, J.L. Perez-Rodriguez, M.L. Franquelo, L.K. Herrera, A. Justo, Determination of pigments and binders in Pompeian wall paintings using synchrotron radiation - high-resolution x-ray powder diffraction and conventional spectroscopy –chromatography, Archaeom. 52 (2) (2010) 286–307.
[20] F. Toschi, A. Paladini, F. Colosi, P. Cafarelli, V. Valentini, M. Falconieri, S. Gagliardi, P. Santoro, A multi-technique approach for the characterization of Roman mural paintings, Appl. Surf. Sci 284 (2013) 291–296.
[21] V. Crupi, V. Allodi, C. Bottari, F. D'Amico, G. Galli, A. Gessini, M.F. La Russa, F. Longo, D. Majolino, G. Mariotto, C. Masciovecchio, A. Pezzino, B. Rossi, S.A. Ruffolo, V. Venuti, Spectroscopic investigation of Roman decorated plasters by combining FT-IR, micro-Raman and UV-Raman analyses, Vibr. Spectr. 83 (2016) 78–84.

[22] F. Toschi, F. Colosi, A. Lentini, A. Paladini, A multidisciplinary study of Roman painted plasters from Roman villa in Ponti Novi (Sabina area, Lazio, Italy), J. Archaeol. Sci. Reports 7 (2016) 114–122.
[23] S.R. Amato, D. Bersani, P.P. Lottici, P. Pogliani, P. Pelosi, A multi-analytical approach to the study of the mural paintings in the presbytery of Santa Maria Antiqua al Foro Romano in Rome, Archaeom. 59 (6) (2017) 1050–1064.
[24] L.D. Mateos, D. Cosano, D. Esquivel, S. Osuna, C. Jiménez-Sanchidrián, Use of Raman microspectroscopy to characterize wall paintings in Cerro de las Cabezas and the Roman villa of Priego de Cordoba (Spain), Vibr. Spectr. 96 (2018) 143–149.
[25] J.S.E. Villar, I. Rodríguez Temiño, H.G.M. Edwards, A. Jiménez Hernández, J.I. Ruiz Cecilia, I. Miralles, The Servilia tomb: an architecturally and pictorially important Roman building, Archaeol Anthropol Sci 10 (2018) 1207–1223, https://doi.org/10.1007/s12520-016-0450-9.
[26] E.J. Cerrato, D. Cosano, D. Esquivel, R. Otero, C. Jiménez-Sanchidrián, J. Rafael Ruiz, A multi-analytical study of a wall painting in the Satyr domus in Córdoba, Spain, Spectrochim. Acta A, 232, (2020) 118148. Doi: Doi: 10.1016/j.saa.2020.118148.
[27] C. Clementi, V. Ciocan, M. Vagnini, B. Doherty, M. Laurenzi Tabasso, C. Conti, B.G. Brunetti, C. Miliani C., Non-invasive and micro-destructive investigation of the Domus Aurea wall painting decorations, Anal. Bioanal. Chem. 401, (2011) 1815–1826. Doi: 10.1007/s00216-011-5250-6.
[28] A. Paradisi, A. Sodo, D. Artioli, A. Botti, D. Cavezzali, A. Giovagnoli, C. Polidoro, M.A. Ricci, Domus aurea, the 'Sala delle maschere': chemical and spectroscopic investigations on the fresco paintings, Archaeometry 54 (6) (2012) 1060–1075, https://doi.org/10.1111/j.1475-4754.2012.00678.x.
[29] M.L. Amadori, S. Barcelli, G. Poldi, F. Ferrucci, A. Andreotti, P. Baraldi, M.P. Colombini, Invasive and non-invasive analyses for knowledge and conservation of Roman wall paintings of the Villa of the Papyri in Herculaneum, Microchem. J. 118 (2015) 183–192, https://doi.org/10.1016/j.microc.2014.08.016.
[30] I. Garofano, J.L. Perez-Rodriguez, M.D. Robador, A. Duran A, An innovative combination of non-invasive UV-Visible-FORS, XRD and XRF techniques to study Roman wall paintings from Sevilla, Spain, J. Cult. Herit., 22, (2016) 1028-1039. http:///dx.doi.org/10.1016/j.culher.2016.07.002.
[31] M. Sbroscia, M. Cestelli-Guidi, F. Colao, S. Falzone, C. Gioia, P. Gioia, C. Marconi, D.Mirabile Gattia, E.M. Loreti, M. Marinelli, M. Missori, F. Persia, L. Pronti, M. Romani, A. Sodo, G. Verona-Rinati, M.A. Ricci, R. Fantoni, Multi-analytical non-destructive investigation of pictorial apparatuses of "Villa della Piscina" in Rome. Microchem. J., 153 (2020) 104450. Doi: 10.1016/j.microc.2019.104450.
[32] A. Dal Fovo, A. Mazzinghi, S. Omarini, E. Pampaloni, C. Ruberto, J. Striova, R. Fontana, Non-invasive mapping methods for pigments analysis of Roman mural paintings, J. Cult. Heritage 43 (2020) 311–318, https://doi.org/10.1016/j.culher.2019.12.002.
[33] M. Vadrucci, A. Mazzinghi, B. Sorrentino, S. Falzone, C. Gioia, P. Gioia, E.M. Loreti, M. Chiari, Characterisation of ancient Roman wall-painting fragments using non-destructive IBA and MA-XRF techniques, X-Ray Spectrom. (2020) 1–11, https://doi.org/10.1002/xrs.3178.
[34] M.F. Alberghina, G. Milazzo, S. Schiavone, L. Randazzo, M. Ricca, N. Rovella, F. Spatafora, E. Fiorenza, M.F. La Russa, The Contribution of Microchemical Analyses and Diagnostic Imaging to the Conservation and Identification of the Degraded Surfaces of Hellenistic-Roman Wall Paintings from Solunto (Sicily), Stud. Cons. (2020), https://doi.org/10.1080/00393630.2020.1805252.
[35] F. Mairinger, The ultraviolet and fluorescence study of paintings and manuscripts, in: D.C. Creagh, D.A. Bradley (Eds.), Radiation in Art and Archeometry, Elsevier Science B.V, 2000, pp. 56–75, https://doi.org/10.1016/B978-044450487-6/50050-X.
[36] J. Warda, F. Frey, D. Heller, D. Kusheld, T. Vitale, G. Weaver, Ultraviolet photography, in: J. Warda (Ed.), AIC guide to digital photography and conservation documentation, American Institute for Conservation of Historic and Artistic Works, Washington, 2011.
[37] J. Dyer, G. Verri, J. Cupitt, Multispectral Imaging in Reflectance and Photo-induced Luminescence modes, A User Manual. (2013) (accessed January 2021) https://www.britishmuseum.org/pdf/charisma-multispectral-imaging-manual-2013.pdf,.
[38] E. K. Webb, UV-Induced Visible Luminescence for Conservation Documentation, in: M. Picollo, M. Stols-Witlox and L. Fuster-López (Eds.), Conservation 360°, UV-Vis luminescence imaging techniques, 1, Editorial Universitat Politècnica de València, 2019, pp. 35-60, Doi: 10.4995/360_2019.110002.
[39] G. Accorsi, G. Verri, M. Bolognesi, N. Armaroli, C. Clementi, C. Miliani, A. Romani, The exceptional near-infrared luminescence properties of cuprorivaite (Egyptian blue), Chem. Commun. (2009) 3392–3394, | doi:10.1039/B902563D http://pubs.rsc.org.
[40] G. Verri, The spatially resolved characterization of Egyptian blue, Han blue and Han purple by photo-induced luminescence digital imaging, Anal. Bioanal. Chem. 394 (2009) 1011–1021, https://doi.org/10.1007/s00216-009-2693-0.
[41] G. Verri, Broad-Band, Photo-Induced, Steady-State Luminescence Imaging in Practice in: M. Picollo, M. Stols-Witlox and L. Fuster-López (Eds.), Conservation 360°, UV-Vis luminescence imaging techniques, 1, Editorial Universitat Politècnica de València, 2019, pp. 61-102, Doi: 10.4995/360_2019.110002.
[42] M. Bacci, Fiber optics applications to works of art, Sens. Actuat. 29 (1995) 190–196.
[43] M. Bacci, UV-VIS-NIR, FT-IR, FORS Spectroscopies, in: E. Ciliberto, G. Spoto (Eds.), Modern Analytical Methods in Art and Archaeology, Chemical Analysis Series, 155, 12, John Wiley and Sons, New York, 2000, pp. 321–362.
[44] M. Aceto, A. Agostino, G. Fenoglio, A. Idone, M. Gulmini, M. Picollo, P. Ricciardi, J. Delaney, Characterisation of colourants on illuminated manuscripts by portable fibre optic UV-Visible-NIR reflectance spectrophotometry, Anal. Methods 6 (5) (2014) 1488, https://doi.org/10.1039/c3ay41904e.
[45] M. Picollo, M. Aceto, T. Vitorino, UV-Vis spectroscopy, in: L. Sabbatini, I.D. van der Werf (Eds.), Chemical Analysis in Cultural Heritage, De Gruyter, Berlin Germany, 2020, pp. 253–271.
[46] IFAC-CNR FORS database Fiber Optics Reflectance Spectra (FORS) of Pictorial Materials in the 270-1700 nm range, http://fors.ifac.cnr.it/index.php (accessed January 2021).
[47] A.G. Karidas, H. Brecoulaki, B. Bourgeois, Ph. Jockey, In situ XRF analysis of raw pigments and traces of polychromy on marble sculpture surfaces. Possibilities and limitations. Non-destructive Examination of Cultural Objects. Advances in X-ray, Analysis (2006) 42–62.
[48] A.N. Shugar, J.L. Mass, Handheld XRF for Art and Archaeology, Leuven University Press, Leuven, 2013.
[49] A. Bezur, L. Lee, Loubser M., K. Trentelman, Handheld XRF in Cultural Heritage, J. Paul Getty Trust and Yale University, 2020.
[50] M. Derrick, L. Souza, T. Kieslich, H. Florsheim, D. Stulik, Embedding paint cross-section samples in polyester resins: Problems and solutions, J. Am. Inst. Conservation 33 (3) (1994) 227–245.
[51] J.J. Hughes, A. B. Leslie, K. Callebaut, The petrography of lime inclusions of historic lime based mortars, in: M. Stamatacis (Ed.), Proceedings of the 8th Euroseminar on Microscopy applied to building materials, Annales Geologiques des pays Helleniques, Athens, 2001, pp. 359-364.
[52] J. Elsen, Microscopy of historic mortars - a review, Cement Concrete Res. 36 (8) (2006) 1416–1424, https://doi.org/10.1016/j.cemconres.2005.12.006.
[53] C. Blaeuer, A. Kueng, Examples of microscopic analysis of historic mortars by means of polarising light microscopy of dispersions and thin sections, Mater. Charact. 58 (2007) 1199–1207, https://doi.org/10.1016/j.matchar.2007.04.023.
[54] S. Pavia, S. Caro, An investigation of Roman mortar technology through the petrographic analysis of archaeological material, Constr. Build. Mater. 22 (8) (2008) 1807–1811, https://doi.org/10.1016/j.conbuildmat.2007.05.003.
[55] J. Weber, W. Prochaska, N. Zimmermann, Microscopic techniques to study Roman renders and mural paintings from various sites, Mater. Charact. 60 (7) (2009) 586–593, https://doi.org/10.1016/j.matchar.2008.12.008.
[56] M. Lezzerini, S. Legnaioli, G. Lorenzetti, V. Palleschi, M. Tamponi, Characterization of historical mortars from the bell tower of St. Nicholas church (Pisa, Italy), Constr. Build. Mater. 69 (2014) 203–212, https://doi.org/10.1016/j.conbuildmat.2014.07.051.
[57] D. Miriello, A. Bloise, G.M. Crisci, R. De Luca, N. Ruggieri, New compositional data on ancient mortars and plasters from Pompeii (Campania – Southern Italy): Archaeometric results and considerations about their time evolution, Mater. Charact. 146 (2018) 189–203, https://doi.org/10.1016/j.matchar.2018.09.046.
[58] E. Pecchioni, F. Fratini, E. Cantisani, Atlante delle malte antiche in sezione sottile al microscopio ottico, 2nd ed., Nardini, Italy, 2017.
[59] G. Paternoster, R. Rinzivillo, F. Nunziata, E,M. Castellucci, C. Lofrumento, M. Zoppi, A.C. Felici, G. Fronterotta, C. Nicolais, M. Piacentini, S. Sciuti, M. Venditelli, Study on the technique of the Roman age mural paintings by micro-XRF with Polycapillary Conic Collimator and micro-Raman analyses, J. Cult. Herit., 6, (2005) 21–28. Doi: 10.1016/j.culher.2004.10.003.
[60] N. Eastaugh, V. Walsh, T. Chaplin, R. Siddall, Pigment Compendium: A Dictionary and optical microscopy of historic pigments, 1st ed.;, Butterworth-Heinemann:, London, UK, 2008, p. 279.
[61] R. Siddall, Mineral Pigments in Archaeology: their analysis and the range of available materials, Minerals 8 (201) (2018) 1–35, https://doi.org/10.3390/min8050201.
[62] M. Elias, C. Chartier, G. Prévot, H. Garay, C. Vignaud, The colour of ochres explained by their composition, Mater. Sci. Eng., B 127 (2006) 70–80, https://doi.org/10.1016/j.mseb.2005.09.061.
[63] B. Weckler, H.D. Lutz, Lattice vibration spectra. Part XCV. Infrared spectroscopic studies on the iron oxide hydroxides goethite (□), akagankite (□), lepidocrocite (□), and feroxyhite (□), Eur. J. Solid State Inorg. Chem. 35 (1998) 531–544.
[64] H. Liu, T. Chen, C. Qing, Q. Xie, R.L. Frost, Confirmation of the assignment of vibrations of goethite: An ATR and IES study of goethite structure, Spectrochim. Acta A 116 (2013) 154–159, https://doi.org/10.1016/j.saa.2013.06.102.
[65] R. Siddal, Not a day without a line drawn: Pigments and painting techniques of Roman Artists. Infocus Magazine, The Proceedings of the Royal Microscopical Society, Oxford, UK, June 2006, (2), 20–31.
[66] I. Aliatis, D. Bersani, E. Campani, A. Casoli, P.P. Lottici, S. Mantovan, I. Marino, Pigments used in Roman wall paintings in the Vesuvian area, J. Raman Spectrosc. 41 (2010) 1537–1542, https://doi.org/10.1002/jrs.2701.
[67] L.D. Mateos, D. Cosano, D. Esquivel, S. Osuna, C. Jiménez-Sanchidrián, Use of Raman microspectroscopy to characterize wall paintings in Cerro de las Cabezas and the Roman villa of Priego de Cordoba (Spain), Vibr. Spectr. 96 (2018) 143–149, https://doi.org/10.1016/j.vibspec.2018.04.004.
[68] L.D. Mateos, D. Cosano, M. Mora, I. Muñiz, R. Carmona, C. Jiménez-Sanchidrián, J.R. Ruiz, Raman microspectroscopic analysis of decorative

pigments from the Roman villa of El Ruedo (Almedinilla, Spain), Spectrochim. Acta A 151 (2015) 16–21, https://doi.org/10.1016/j.saa.2015.06.091.
[69] E.J. Cerrato, D. Cosano, D. Esquivel, R. Otero, C. Jiménez-Sanchidrián, J.R. Ruiz, A multi-analytical study of a wall painting in the Satyr domus in Córdoba, Spain, Spectrochim. Acta A 232 (2020), https://doi.org/10.1016/j.saa.2020.118148 118148.
[70] F. Agnoli, I. Calliari, G. Mazzocchin, Use of different spectroscopic techniques in the analysis of Roman age wall paintings, Anal. Chim. 97 (2007) 1–7.
[71] R. Piovesan, R. Siddall C. Mazzoli, L. Nodari, The Temple of Venus (Pompeii): a study of the pigments and painting techniques, J. Archaeol. Sci., 38 (2011) 2633-2643. https://doi.org 10.1016/j.jas.2011.05.021.
[72] C. Genestar, C. Pons, Earth pigments in painting: characterisation and differentiation by means of FTIR spectroscopy and SEM-EDS microanalysis, Anal. Bioanal. Chem. 382 (2005) 269–274, https://doi.org/10.1007/s00216-005-3085-8.
[73] L.R. Marshall, J.R. Williams, M.J. Almond, S.D.M. Atkinson, S.R. Cook, W. Matthews, J.L. Mortimore, Analysis of ochres from Clearwell Caves: the role of particle size in determining colour, Spectrochim. Acta A 61 (2005) 233–241. Doi: 10.1016/j.saa.2004.03.041.
[74] A. Maras, M. Botticelli, P. Ballirano, Archaeometric investigations on cinnabar provenance and origin by X-ray powder diffraction: preliminary data, Int. J. Cons. Sci 4 (2013) 685–692.
[75] D. Damiani, E. Gliozzo, I. Memmi Turbanti, J.E. Spangenberg, Pigments and plasters discovered in the House of Diana (Cosa, Grosseto, Italy): an integrated study between art history, archaeology and scientific analyses, Archaeom. 45 (2) (2003) 341–354, https://doi.org/10.1111/1475-4754.00112.
[76] G.A. Mazzocchin, P. Baraldi, C. Barbante, Isotopic analysis of lead present in the cinnabar of Roman wall paintings from the Xth Regio "(Venetia et Histria)" by ICP-MS, Talanta 74 (2008) 690–693, https://doi.org/10.1016/j.talanta.2007.06.048.
[77] M.K. Neiman, M. Balonis, J. Kakoulli, Cinnabar alteration in archaeological wall paintings: an experimental and theoretical approach, Appl. Phys. A 121 (2015) 915–938, https://doi.org/10.1007/s00339-015-9456-x.
[78] P. Baraldi, C. Baraldi, R. Curina, L. Tassi, P. Zannini, A micro-Raman archaeometric approach to Roman wall paintings, Vib. Spectr. 43 (2007) 420–426, https://doi.org/10.1016/j.vibspec.2006.04.029.
[79] P. Vandenabeele, K. Lambert, S. Matthys, W. Schudel, A. Bergmans, L. Moens In situ analysis of mediaeval wall paintings: a challenge for mobile Raman spectroscopy. Anal Bioanal Chem., 383, (2005) 707–712. Doi: 10.1007/s00216-005-0045-2.
[80] J.K. McCormack, The darkening of cinnabar in sunlight, Miner. Deposita 35 (2000) 796–798.
[81] M. Cotte, J. Susini, J. Dik, K. Janssens, Synchrotron-based X-ray absorption spectroscopy for art conservation: looking back and looking forward, Acc. Chem. Res. 43 (6) (2010) 705–714, https://doi.org/10.1021/ar900199m.
[82] M. Spring, R. Grout, The blackening of vermilion: an analytical study of the process in paintings, Nat. Gall. Techn. Bull. 23 (2002) 50–61.
[83] M. Cotte, J. Susini, N. Metrich, A. Moscato, C. Gratziu, A. Bertagnini, M. Pagano, Blackening of pompeian cinnabar paintings: X-ray microspectroscopy analysis, Anal. Chem. 78 (2006) 7484–7492, https://doi.org/10.1021/ac0612224.
[84] C. Hogan, F. Da Pieve, Colour degradation of artworks: an ab initio approach to X-ray, electronic and optical spectroscopy analyses of vermilion photodarkening, J. Anal. At. Spectrom. 30 (2015) 588–598, https://doi.org/10.1039/c4ja00327f.
[85] H. Béarat, Les pigments verts en peinture murale romaine: bilan analytique, in: H. Béarat, M. Fuchs, M. Maggetti, D. Paunier (Eds.), Proceedings of the International Workshop on Roman Wall Painting, Institute of Mineralogy and Petrology, Fribourg, 1996, pp. 269–286.
[86] I. Marcaida, M. Maguregui, H. Morillas, N. Prieto-Taboada, S. Fdez-Ortiz de Vallejuelo, M. Veneranda, J.M. Madariaga, A. Martellone, B. De Nigris, M. Osanna, In situ non-invasive characterization of the composition of Pompeian pigments preserved in their original bowls, Microchem. J. 139 (2018) 458–466, https://doi.org/10.1016/j.microc.2018.03.028.
[87] R. Debastiani, R. Simon, J. Goettlicher, S. Heissler, R. Steininger, D. Batchelor, M. Fiederle, T. Baumbach, Identification of green pigments from fragments of Roman mural paintings of three Roman sites from north of Germania Superior, Appl. Phys. A 122 (871) (2016) 1–12, https://doi.org/10.1007/s00339-016-0400-5.
[88] J.L. Perez-Rodriguez, M. Jimenez de Haro, B. Siguenza, J.M. Martinez-Blanes, Green pigments of Roman mural paintings from Seville Alcazar, Appl. Clay Sci. 116–117 (2015) 211–219, https://doi.org/10.1016/j.clay.2015.03.016.
[89] M.C. Caggiani, A. Coccato, P. Mazzoleni, A. D'Alessio, A. Russo, G. Barone G., Integrated analytical approach to unveil the secrets of the recently discovered "Sphinx Room": a new piece of Domus Aurea puzzle, Herit. Sci., 8:124, (2020) 1-21. Doi: 10.1186/s40494-020-00465-1.
[90] J.M. Malézieux, B. Piriou, Relation entre la composition chimique et le comportement vibrationnel de spinelles de synthèse et de chromites naturelles en microspectrométrie Raman, Bull. Minér. 111 (6) (1988) 649–669, https://doi.org/10.3406/bulmi.1988.8110.
[91] C.A. Grissom, Green earth, in: R.L. Feller (Ed.), Artists' Pigments, vol. 1, UK, Cambridge University Press, 1986, p. 141.
[92] F. Ospitali, D. Bersani, G. Di Lonardo, P.P. Lottici, 'Green earths': vibrational and elemental characterization of glauconites, celadonites and historical pigments, J. Raman Spectrosc. 39 (2008) 1066–1073, https://doi.org/10.1002/jrs.1983.
[93] I. Aliatis, D. Bersani, E. Campani, A. Casoli, P.P. Lottici, S. Mantovan, I. Marino, F. Ospitali, Green pigments of the Pompeian artists'palette, Spectrochim. Acta A 73 (2009) 532–538, https://doi.org10.1016/j.saa.2008.11.009.
[94] L.M. Moretto, E.M. Orsega, G.A. Mazzocchin, Spectroscopic methods for the analysis of celadonite and glauconite in Roman green wall paintings, J. Cult. Herit. 12 (2011) 384–391, https://doi.org/10.1016/j.culher.2011.04.003.
[95] A. Fanost, A. Gimata, L. de Vigueriea, P. Martinetto, A. Giota, M. Clemanceye, G. Blondine, F. Gaslain, H. Glanvillea, P. Waltera, G. Meriguet, A. Rollet, M. Jabera, Revisiting the identification of commercial and historical green earth pigments, Colloids Surf. A 584 (2020), https://doi.org/10.1016/j.colsurfa.2019.124035 124035.
[96] G.A. Mazzocchin, E. F. Orsega, P. Baraldi, P. Zannini, Aragonite in Roman wall paintings of the VIIIa Regio Aemilia, and Xa Regio, Venetia et Histria, Annali di Chimica, 96, (2006) 377-387.
[97] G.A. Mazzocchin, A. Vianello, S. Minghelli, D. Rudello, Analysis of roman wall paintings from the thermae of 'Iulia Concordia', Archaeom. 52 (4) (2010) 644–655, https://doi.org/10.1111/j.1475-4754.2009.00501.x.
[98] IRUG database, Infrared & Raman Users Group. http://www.irug.org/. (accessed January 2021).
[99] G.A. Mazzocchin, F. Agnoli, S. Mazzocchin, I. Colpo, Analysis of pigments from Roman wall paintings found in Vicenza, Talanta 61 (2003) 565–572, https://doi.org/10.1016/S0039-9140(03)00323-0.
[100] M. Gutman, M. Lesar Kikelj, B. Zupanek, S. Kramar, Wall paintings from the roman Emona (Ljubljana, Slovenia): characterization of mortar layers and pigments, Archaeom. 58 (2) (2016) 297–314, https://doi.org/10.1111/arcm.12167.
[101] I. Riederer, Egyptian blue, in E. West Fitzhugh (Ed). , Artists' Pigments, vol. 3, Cambridge University Press: UK, 1997; 23-46.
[102] D.A. Scott, Egyptian blue and other synthetic copper silicates, in: Copper and Bronze in art – Corrosion, colorants, conservation. The Getty Conservation Institute (LA, USA), 2002, 257-267.
[103] R. Piovesan, C. Mazzoli, L. Maritan, P. Cornale, Fresco and lime paint: an experimental study and objective criteria for distinguishing between these painting techniques, Archaeom. 54 (4) (2012) 723–736, https://doi.org/10.1111/j.1475-4754.2011.00647.x.
[104] I. Regazzoni, G. Cavallo, D. Biondelli, J. Gilardi, Microscopic analysis of wall painting techniques: laboratory replicas and romanesque case studies in southern switzerland, Stud. Conserv. 63 (6) (2018) 326–341, https://doi.org/10.1080/00393630.2017.1422891.
[105] G. Allag, S. Groetembril, 2021, Le rôle des sous-couches, in M. Cavalieri, P. Tomassini (Eds.), La peinture murale antique, méthodes apports d'une approche technique, Actes du colloque international de Louvain-la-Neuve, 21 Avril 2017 (AIRPA), Rome, 202, 205-212.
[106] A. Barbet, La technique comme revelateur d'écoles, de modes, d'individualités des pentre?, Mededelingen Rom (1995) 61–78
[107] A. Barbet, L'emploi des couleurs dans la peinture murale romaine antique : « Marqueurs » chronologiques et révélateurs du « standing » social ? In : Pigments et colorants de l'Antiquité et du Moyen Âge : Teinture, peinture, enluminure, études historiques et physico-chimiques CNRS Éditions, Paris, 2002. Doi: 10.4000/books.editionscnrs.8180.
[108] S. Bracci, E. Cantisani, Analyses of microsamples from the archeological site of Agios Donatos (GR), ICVBC Scientific Report (2012), not published.
[109] A. Freccero, The Roman villa of Agios Donatos. Fragments of wall painting, in: B.Forsén (ed.), Thesprotia Expedition IV. Region Transformed by Empire, Papers and Monographs of the Finnish Institute at Athens, Helsinki, vol. XXIV, 2019, 275-298.